

Original Manuscript

A panel of *in vitro* tests to evaluate genotoxic and morphological neoplastic transformation potential on *Balb/3T3* cells by pristine and remediated titania and zirconia nanoparticles

Andrea Stoccoro^{1,2}, Sebastiano Di Bucchianico^{1,6}, Chiara Ubaldi^{1,7},
Fabio Coppedè¹, Jessica Ponti³, Claudia Placidi⁴, Magda Blosi⁵,
Simona Ortelli⁵, Anna Luisa Costa⁵ and Lucia Migliore^{1,*}

¹Laboratory of Medical Genetics, Department of Translational Research and New Technologies in Medicine and Surgery, University of Pisa, Via Roma 55, Pisa 56126, Italy, ²Doctoral School in Genetics, Oncology and Clinical Medicine, Department of Medical Biotechnologies, University of Siena, 53100 Siena, Italy, ³European Commission, Joint Research Centre (JRC), Institute for Health and Consumer Protection (IHCP), Nanobiosciences (NBS) Unit, via E. Fermi 2749, 21027 Ispra (VA), Italy, ⁴Department of Pathology, Ospedale di Circolo and Department of Human Morphology, University of Insubria, via Ottorino Rossi 9, 21100 Varese, VA, Italy and ⁵Institute of Science and Technology for Ceramics (CNR-ISTEC), National Research Council of Italy, Via Granarolo 64, 48018 Faenza, RA, Italy

⁶Present address: Division of Biochemical Toxicology, Institute of Environmental Medicine, Karolinska Institutet, Stockholm, Sweden.

⁷Present address: Biogenotoxicology, Human Health and Environment Unit, Mediterranean Institute of Marine and Terrestrial Biodiversity and Ecology (IMBE), Aix-Marseille University, Marseille, France.

*To whom correspondence should be addressed. Tel: +39 050 2218549; Fax: +39 050 2210624; Email: lucia.migliore@med.unipi.it

Received 12 January 2016; Revised 25 February 2016; Accepted 7 March 2016.

Abstract

The FP7 Sanowork project was aimed to minimise occupational hazard and exposure to engineered nanomaterials (ENM) through the surface modification in order to prevent possible health effects. In this frame, a number of nanoparticles (NP) have been selected, among which zirconium (ZrO_2) and titanium (TiO_2) dioxide. In this study, we tested ZrO_2 NP and TiO_2 NP either in their pristine (uncoated) form, or modified with citrate and/or silica on their surface. As benchmark material, Aeroxide® P25 was used. We assessed cytotoxicity, genotoxicity and induction of morphological neoplastic transformation of NP by using a panel of *in vitro* assays in an established mammalian cell line of murine origin (Balb/3T3). Cell viability was evaluated by means of colony-forming efficiency assay (CFE). Genotoxicity was investigated by cytokinesis-block micronucleus cytome assay (CBMN cyt) and comet assay, and by the use of the restriction enzymes EndoIII and Fpg, oxidatively damaged DNA was detected; finally, the morphological neoplastic transformation of NP was assayed *in vitro* by cell transformation assay (CTA). Our results show that the surface remediation has not been effective in modifying cyto- and genotoxic properties of the nanomaterials tested; indeed, in the case of remediation of zirconia and titania with citrate, there is a tendency to emphasise the toxic effects. The use of a panel of assays, such as those we have employed, allowing the evaluation of multiple endpoints, including cell transformation, seems particularly advisable especially in the case of long-term exposure effects in the same cell type.

Introduction

The research on engineered nanomaterials (ENM) and the design of synthetic methods for their production has seen an enormous improvement during the last decade, originating from potential applications of these systems in a wide variety of attractive fields, ranging from communications and microelectronics to medical diagnostics and therapy (1).

Despite of the large amount of available literature on these themes, the production of engineered nanoparticles (NP) with a high control degree over their chemicophysical and functional properties remains a hot topic in materials science (2).

The possible impact on human health of NP is until now not well understood. Several authors have suggested that NP can be toxic to various human organs and systems, inducing complex pathologies such as cancer (3) and neurodegenerative diseases (4).

The FP7 Sanowork project was aimed to minimise occupational hazard and exposure to ENM through their surface modification in order to prevent possible deleterious health effects.

Different 'design option'-based risk remediation strategies focused on ENM surface engineering have been proposed and integrated within various ENM manufacturing processing lines, becoming process extra-steps to be evaluated in terms of risk and expected performances.

In this frame, a number of ENM have been selected, among which ZrO_2 and TiO_2 NP have been collected, modified and investigated in this study.

In order to control and decrease the potential toxicity and emission of ZrO_2 and TiO_2 NP, two different approaches for surface modification were employed: an inorganic inert coating (SiO_2 NP), added by means of a heterocoagulation and an organic coating citrate-based, applied by using a self-assembling strategy. The process line involving ZrO_2 NP was focused on the washing step of industrial reactors employed for synthesising ZrO_2 by sol gel reaction. The critical step to be monitored for its potential exposure was referred to the washing of the synthetic reactor. During this step, the proposed risk remediation strategies had the potentiality to improve the washing efficiency by improving ZrO_2 water dispersion and so decreasing environmental emission potential. The target TiO_2 NP sample studied was involved in the processing line consisting in the application of TiO_2 nanosols to ceramic substrates through spray coating, one of the most flexible methods for the application of nanostructured suspensions, allowing rapid and simple production changes. The critical step for health hazard and exposure assessment was actually the spray coating operation which could cause nanoaerosolisation and induce inhalation of NP. SiO_2 and citrate coatings were proposed for both nano metal oxides investigated in the present study for their potential to improve powder dispersability and hydrophylicity, positively impacting on mechanism driving cellular toxicity (5).

To investigate the cytotoxic, genotoxic and morphological neoplastic potential of the pristine and modified ZrO_2 and TiO_2 NP, we used a panel of assays including the colony formation efficiency test (CFE), the cytokinesis-block micronucleus cytome assay (CBMN cyt), the comet assay and the cell transformation assay (CTA) in Balb/3T3 mouse fibroblasts. The choice of the cell line was driven by the availability of the *in vitro* CTA limited to few cell types. After exposure to carcinogens, Balb/3T3 cells become tumorigenic forming morphologically transformed colonies (foci type III). Their ability to induce cancer *in vivo* is detectable by injecting the transformed cells in nude mice and observing their growth as sarcomas (6,7).

Methods

Preparation and characterisation of ZrO_2 and TiO_2 NP

Commercial ZrO_2 and TiO_2 (84% anatase, 16% brookite crystal phase composition, 8), NP were provided by PlasmaChem GmbH (Germany) as nanopowder and by Colorobbia Italia SpA as colloidal nanosuspension (nanosol), respectively.

For ZrO_2 and TiO_2 NP, the remediation process consisted in silica and sodium citrate coating. The following panel of NP were thus studied: pristine ZrO_2 , citrate-coated ZrO_2 (low and high citrated), silica-coated ZrO_2 , pristine TiO_2 , citrate-coated TiO_2 and silica-coated TiO_2 . Furthermore, TiO_2 Aerioxide® P25 were used as benchmark material.

ZrO_2 nanosols preparation

The process line involving ZrO_2 NP is focused on the washing step of industrial reactors employed for synthesizing ZrO_2 by sol gel reaction. Two kinds of surface modifications were aimed at improving ZrO_2 NP dispersion: an inorganic inert coating (SiO_2 NP) by means of a heterocoagulation approach and an organic coating citrate-based by using a self-assembling strategy.

ZrO_2 NP provided by PlasmaChem as nanopowder was suspended in water with a solid loading of 3% wt. The resulting suspension (pristine), highly stable, was used as starting material for the subsequent modifications.

Modified sample labelled as ZrO_2 silica coated NP, was obtained by mixing pristine ZrO_2 nanosol with commercial colloidal SiO_2 (Ludox S40) in a proper weight ratio ($\text{SiO}_2:\text{ZrO}_2 = 4:1$) keeping a total solid loading of 3% wt. Then, in order to promote the heterocoagulation process, the so prepared sample was ball milled for 24 h.

Samples modified with the organic layer were prepared by adding trisodium citrate dihydrate to the pristine then ball milling for 24 h. Two different weight ratios were produced ($\text{ZrO}_2:\text{Cit} = 1:0.01$ and 1:1) keeping the total solid concentration at 3% wt, the so prepared samples were named, respectively, low-citrate and high-citrate coated NP.

TiO_2 nanosols preparation

The silica modified TiO_2 NP were produced following the heterocoagulation route: opposite charged TiO_2 NP and SiO_2 NP were diluted and then mixed together at room temperature, maintaining a $\text{SiO}_2/\text{TiO}_2$ weight ratio equal to 3 and a total solid content of 3% wt. The obtained mixtures were ball milled for 24 h using 5 mm diameter zirconia spheres as milling media to obtain slightly cloudy solutions.

The citrate modified TiO_2 NP were produced by self-assembly strategy: trisodium citrate dihydrate was added to a previously diluted TiO_2 NP suspension at room temperature and employing a citrate/ TiO_2 NP weight ratio equal to 0.83. The reaction mixture was stirred overnight resulting in a transparent and stable suspension.

Sol state characterisation of ZrO_2 and TiO_2 NP

The chemicophysical characterisation of the pristine and modified ZrO_2 and TiO_2 samples was performed by means of transmission electron microscopy (TEM), dynamic light scattering (DLS) and Z-potential.

The morphological analysis on pristine and modified samples was performed by FEI titan TEM operating at an acceleration voltage of 300kV. One drop of diluted NP suspension in deionised water (30 $\mu\text{g}/\text{ml}$) was deposited on a film-coated copper grid and characterised.

Hydrodynamic diameter of ZrO_2 and TiO_2 (pristine and modified forms) were investigated for samples dispersed both in deionised water and complete cell culture medium (125 $\mu\text{g}/\text{ml}$) using light scattering optical technique (Zetasizer nano ZSP model ZEN5600; Malvern Instruments, UK).

NP hydrodynamic diameter (d DLS) was obtained from DLS data, setting the measurement angle to 173° and the measurement duration on automatic. After 2 min temperature equilibration step, 1 ml of sample volume was subjected to three consecutive measurements performed at 25°C and particle size distributions by intensity were obtained by averaging these measurements.

The colloidal stability in medium was evaluated by repeating measurements at $t = 0$ –72 h. The standard operating procedure described hereafter was followed for all samples. At $t = 0$ h, each stock suspension was sonicated for 15 min and aliquots were first added to 0.05% (v/v) BSA/PBS to obtain an intermediate which was then added to MEM (Minimum Essential Medium, Gibco) culture medium supplemented with 10% (v/v) serum to reach a final ZrO_2 and TiO_2 concentration of 125 $\mu\text{g}/\text{ml}$. For analyses at $t = 24$, 48, 72 h, samples were thermostated at 37°C.

After particle size determination, samples underwent Zeta potential measurement by electrophoretic light scattering (ELS). The Smoluchowski approximation, consistent with the high dielectric constant of water that is the main component of the all above specified solvents, was applied to convert the electrophoretic mobility to zeta potential. Zeta potential measurements were performed on 700 μl of volume sample at 25°C. Before and after zeta potential analyses a size measurement was performed to check that the samples have not changed. The measurement data of samples dispersed in MEM culture medium were collected in monomodal mode due to the high medium conductivity (approximately thus obtaining a mean zeta potential value). The amount of BSA added was calculated as well as a function of powder surface, carrying out specific surface area (BET) measurements on the dried powders using N_2 as adsorptive gas Sorpty 1750 (Carlo Erba, Italy). The specific surface area (SSA) measurements were determined by Brunauer–Emmett–Teller (BET) method. It is a well-recognised approach to determine the specific surface area of nanoporous materials which is based on physical adsorption of gas molecules (N_2) onto the material interface (9,10). The specific surface area (BET) measurements were carried out using N_2 as adsorptive gas Sorpty 1750 (Carlo Erba, Italy).

Zeta potential of nanosols as a function of pH (experimental uncertainty: 3 mV for Z potential and 0.03 for pH) was measured with an electroacoustic technique (AcoustoSizer II, Colloidal Dynamics, Australia, equipped with an automatic titrating system) that allowed identify the point of zero Z-potential (isoelectric point, i.e.p.). The measurements were carried out on aqueous solutions at 10 mg/mL KOH 1M and HCl 1M were used to modify pH within 2–8 pH range.

Cell culture conditions

Balb/3T3 mouse fibroblasts were supplied at passage 13 from the Hatano Research Institute, Japan. Experimental cultures were prepared from deep-frozen stock vials and always kept in a subconfluent state. They were maintained in complete culture medium prepared using Minimum Essential Medium with Earle's salts and l-glutamine (MEM) supplemented with 1% v/v of penicillin/streptomycin (10⁴ Units/ml), 10% v/v of Fetal Bovine Serum New Zealand Origin (Moregate, lot. number 47827101), and passaged at 1:15 ratio, using trypsin-EDTA (Gibco). Cell preparations were maintained in standard cell culture conditions (37°C, 5% CO_2 and 95% humidity) no longer than 10 passages.

In order to identify the most suitable concentrations to use in genotoxicity assays and in CTA assay, we previously have investigated the effect of a wide range of NP doses on Balb/3T3 cell viability by means of CFE assay. For this purpose, we treated the cells with NP concentrations ranging from 1.25 to 80 $\mu\text{g}/\text{cm}^2$, corresponding to a range of 8.3–266.6 $\mu\text{g}/\text{ml}$, a range of doses representative of realistic human exposure (11). In this way, the concentrations of 10, 20 and 40 $\mu\text{g}/\text{cm}^2$ were selected, excluding the concentration of 80 $\mu\text{g}/\text{cm}^2$ since at this concentration NP caused a marked turbidity of the medium. For cellular uptake study, we have chosen the intermediate time and concentration used in genotoxicity and cell transformation investigations.

ZrO_2 and TiO_2 NP internalisation in Balb/3T3 cells

To study NP cell internalisation, Balb/3T3 cells were seeded in 75 cm² flasks (Corning Costar, Italy) at a density of 2.5×10^5 cells in 10 ml of complete cell culture medium. After 24 h, cells were exposed to 20 $\mu\text{g}/\text{cm}^2$ of ZrO_2 and TiO_2 NP for 48 h. After exposure, medium was removed and cells were thoroughly washed with PBS, detached using 1 ml trypsin-EDTA (Invitrogen, Italy) and centrifuged at 200 $\times g$ for 5 min to obtain the cell pellet. The supernatant was removed and cells were fixed using a Karnovsky 2% v/v solution (glutaraldehyde and paraformaldehyde in 0.05 M cacodilate buffer at pH 7.3, Sigma Aldrich, Italy) over night. Cells were then washed three times with 0.05 M cacodilate, pH 7.3 (Sigma Aldrich, Italy) and post-fixed in osmium tetroxide solution in 0.1 M pH 7.3 cacodilate (Sigma Aldrich, Italy) for 1 h; after 3 additional washes in 0.05 M cacodilate of 10 min each cells were dehydrated in a graded series of ethanol solution in MilliQ water (30%; 50%; 75%; 95% for 15 min each, and 100% for 30 min), incubated in absolute propylene oxide (Sigma Aldrich, Italy) for 20 min (2 changes of 10 min each) and embedded in a solution of 1:1 epoxy resin (Sigma Aldrich, Italy) and propylene oxide for 90 min. This mixture was renewed with pure epoxy resin (Sigma Aldrich, Italy) over night at room temperature, and later polymerised at 60°C for 48 h. Ultrathin sections (60–90 nm) were obtained using Leica UCT ultramicrotome (Leica, Italy) and stained for 25 min with uranyl acetate (Sigma Aldrich, Italy) and lead citrate for 20 min, washed and dried. Ultrathin sections were imaged under 80 kV Philips 208 TEM.

Concurrent cytotoxicity and morphological transformation assay

The Balb/3T3 CTA has been carried out by assessing the concurrent cytotoxicity and morphological neoplastic transformation in terms of colony-forming efficiency (CFE) and formation of type-III foci, respectively.

Colony-forming efficiency assay

CFE assay was performed as detailed elsewhere (12) to study the cytotoxicity induced by ZrO_2 and TiO_2 NP at 24, 48 and 72 h of exposure. Cells were seeded at the density of 200 cells per dish in 3 ml complete culture medium (60 × 15 mm Petri dish, 20 cm² bottom surface area, BD FalconTM). After 24 h, NP suspensions were directly added to the cell culture to obtain the appropriate final ZrO_2 and TiO_2 NP concentrations ranging from 1.25 to 80 $\mu\text{g}/\text{cm}^2$, corresponding to a range of 8.3–266.6 $\mu\text{g}/\text{ml}$. Negative (untreated cells) and positive (Na_2CrO_4 1000 μM) were also included. After 24, 48 or 72 h of exposure, the medium was changed with fresh complete culture medium, and 7 days later, the cells were fixed with 3.7% (v/v) of formaldehyde solution (Sigma-Aldrich, Milan, Italy) in phosphate-buffered saline (PBS) (1×) without calcium, magnesium and sodium

bicarbonate (Gibco), and stained with 0.4% (v/v) Giemsa solution (Sigma-Aldrich) in ultrapure water. Colonies were manually scored under a stereomicroscope.

The results are expressed as CFE (%) = [(average of treatment colonies/average of control colonies) \times 100] and the corresponding standard error mean [SEM % = SD/ \sqrt{n} (number of treatments)].

CTA

CTA was performed to investigate if tested NP were able to induce morphological neoplastic transformation in Balb/3T3 fibroblasts. CTA is considered a powerful tool to investigate *in vitro* the morphological neoplastic transformation induced by both genotoxic and non-genotoxic carcinogens as reported in OECD guidelines (13).

CTA was carried out as reported elsewhere (12,14) on Balb/3T3 cells treated with ZrO_2 and TiO_2 NP at concentration of 10, 20 and 40 $\mu\text{g}/\text{cm}^2$, corresponding to 91.6, 183.3 and 366.6 $\mu\text{g}/\text{ml}$, respectively. Non-treated Balb/3T3 cells and cells exposed to 4 $\mu\text{g}/\text{ml}$ methylcholanthrene (MCA, Sigma-Aldrich; Saint Louis, MO, USA), which is a well-known carcinogenic compound, were used as negative and positive controls, respectively.

On day zero, 2×10^4 Balb/3T3 cells were seeded in 100 mm-Petri dish (100 \times 20 mm, 55 cm^2 bottom surface area, BD Falcon™) in 6 ml of complete fresh medium Minimum Essential Medium (MEM) 1x supplemented with 10% (v/v) fetal bovine serum New Zeland origin (Moregate, lot. number 47827101) and 1% v/v antibiotics (10 000 U/ml penicillin and 10 000 $\mu\text{g}/\text{ml}$ streptomycin); 5 replicates per concentration were prepared. At the end of exposure (72 h), medium containing NP was removed and replaced with Dulbecco's modified Eagle's medium/F12 (DMEM/F12) with high glucose, l-glutamine (365 mg/l) and sodium bicarbonate (1200 mg/l) (Invitrogen; Carlsbad, CA, USA) supplemented with 2% (v/v) fetal bovine serum New Zeland origin (Moregate, lot. number 47827101), 2 $\mu\text{g}/\text{ml}$ insulin (Sigma-Aldrich; Saint Louis, MO, USA) and 1% v/v antibiotics (10 000 U/ml penicillin and 10 000 $\mu\text{g}/\text{ml}$ streptomycin) (Invitrogen; Carlsbad, CA, USA). The culture medium was changed twice a week, and on days 31–35 cells were fixed with 4% (v/v) of formaldehyde in PBS. Subsequently, cells were stained with a 10% (v/v) Giemsa solution in ultrapure water. The dishes were air-dried and observed using a stereomicroscope (Olympus; Milan, Italy) in order to detect and count the morphologically transformed colonies (type-III foci), as described from the International Agency for Cancer Research (IARC) Working-Group (W.g. IARC/NCI/EPA, 1985).

Transformation results were expressed as transformation frequency (Tf) (five replicates per concentration, three experiments performed) using the following formula: Tf = A/B; where: A = total number of type III foci counted in each treatment, B = number of surviving cells corresponding to $[(2 \times 10^4) \times 5 \text{ dishes} \times \text{CFE}\%]/100 \times (\text{plating efficiency}/100)$, where: 2×10^4 = number of cells seeded per dish and plating efficiency = (number of colonies formed in the control/number of cells seeded in each CFE dish) \times 100.

Cytokinesis-block micronucleus cytome assay

CBMN cyt was performed according to the procedure described by Di Buccianico and coauthors (15). A total of 7.5×10^5 cells were seeded in six-well cell culture plates (9.6 cm^2 bottom surface area, Falcon™) and after 24 h of culture, the cells were exposed to ZrO_2 and TiO_2 NP at the concentrations of 10, 20 and 40 $\mu\text{g}/\text{cm}^2$, corresponding to 32, 64 and 128 $\mu\text{g}/\text{ml}$, respectively, for 48 h. Mitomycin C (0.1 $\mu\text{g}/\text{ml}$; MMC, Kyowa Hakko Kogyo Co, Chiyoda, Tokyo, Japan) as positive control was used. Cytochalasin B (6 $\mu\text{g}/\text{ml}$) was

added after 44 h to block the cytokinesis process and cells were harvested after 72 h.

The parameters evaluated were the cytokinesis-block proliferation index (CBPI) and the replication index (RI) to test the cytostasis and the apoptotic and necrotic indices to investigate the cytotoxicity exerted by ZrO_2 and TiO_2 NP in the first 500 cells counted. The genotoxic potential was evaluated by scoring the micronucleus (MN) frequency on 1000 binucleated cells. On these 1000 binucleated cells other parameters such as nucleoplasmic bridges (NPB), a biomarker of DNA misrepair and/or telomere end-fusions, and nuclear buds (NBUD), a biomarker of elimination of amplified DNA and/or DNA repair complexes, were also scored as previously described (15,16).

Comet assay

The modified alkaline comet assay was carried out on Balb/3T3 cell cultures seeded at a concentration of 7×10^4 cells/ cm^2 in six-well cell culture plates (9.6 cm^2 bottom surface area, Falcon™) by using the Comet Assay kit following the manufacturer's instructions (Trevigen, Gaithersburg, MD, USA). After 24 h, cells were treated with ZrO_2 and TiO_2 NP at 10, 20 and 40 $\mu\text{g}/\text{cm}^2$, corresponding to 32, 64 and 128 $\mu\text{g}/\text{ml}$, respectively, for 2, 24, 48 and 72 h. The percentage of total DNA fluorescence in tail in a total of 100 randomly selected cells per sample (two replicates, each with 50 cells/slide) was used as a measure of the amount of primary DNA damage. Untreated cells (negative control) and cells exposed for 5 min to H_2O_2 (50 μM) as positive control were used. To determine the

Table 1. Mean hydrodynamic size by intensity and Zeta potential for 125 $\mu\text{g}/\text{ml}$ of uncoated, silicated and citrated ZrO_2 NP, dispersed in deionized water and complete culture medium

ZrO_2 NP	Deionized water			
	pH	Z-pot (mV)	Mean size (nm)	PdI
Uncoated	3.6	41.0 ± 2.0	261 ± 79	0.36 ± 0.08
Silicated	4.6	-40.4 ± 1.8	276 ± 85	0.38 ± 0.08
Low citrated	3.4	40.3 ± 2.7	83 ± 32	0.76 ± 0.22
High citrated	6.5	-47.0 ± 0.0	173 ± 13	0.39 ± 0.08
Complete culture medium				
Uncoated				
0 h	7.4	-11.7 ± 0.3	1537 ± 84	1.00 ± 0.00
24 h		-10.9 ± 0.4	1376 ± 460	0.84 ± 0.28
48 h		-10.8 ± 0.4	941 ± 141	1.00 ± 0.00
72 h		-11.0 ± 0.4	444 ± 50	0.88 ± 0.21
Silicated				
0 h	7.3	-11.0 ± 0.5	244 ± 9	0.99 ± 0.02
24 h		-10.2 ± 0.4	172 ± 3	1.00 ± 0.00
48 h		-11.2 ± 0.5	141 ± 3	0.59 ± 0.04
72 h		-10.9 ± 0.7	101 ± 1	0.54 ± 0.01
Low citrated				
0 h	7.3	-11.9 ± 0.6	1950 ± 1018	0.99 ± 0.02
24 h		-10.9 ± 0.3	1713 ± 236	0.79 ± 0.20
48 h		-11.0 ± 1.4	1530 ± 293	0.80 ± 0.21
72 h		-11.2 ± 0.2	1239 ± 49	0.96 ± 0.07
Ultrafiltered ^a				
8.20		-22.1 ± 0.7		
High citrated				
0 h	7.4	-10.3 ± 0.4	26 ± 0	0.68 ± 0.01
24 h		-11.1 ± 0.1	36 ± 0	0.47 ± 0.00
48 h		-11.20 ± 0.55	55 ± 1	0.47 ± 0.04
72 h		-11.20 ± 0.50	62 ± 1	0.42 ± 0.06

Data are reported as the mean \pm SD. PdI, polydispersity index.

^a ZrO_2 NP extracted by ultrafiltration from complete culture medium and redispersed in water.

presence of oxidised pyrimidine and purine bases, after 2 and 24h of treatment, Endonuclease III (EndoIII) and Formamidopyrimidine-DNA Glycosylase (Fpg) enzymes were used. To determine the number of enzyme-sensitive sites, the difference between the value of the percent of DNA fluorescence in tail obtained after digestion with each enzyme and with the buffer only was calculated. Three independent experiments were performed for each treatment by avoiding direct light exposures of preparing slides. Analysis was carried out by using a Comet Image Analysis System, version 5.5 (Kinetic Imaging, Nottingham, UK).

Statistical analysis

Statistical analysis was performed using GraphPad Prism software. Data of toxicological assays were presented as the mean \pm SEM. Since no difference was observed between negative and solvent control (ultrapure water) for NP, statistical analysis was performed only to evaluate differences between negative control and NP treated cells. The approach to test statistical significance of differences between negative control and NP-treated groups for the CFE assay, CBMN cyt assay and comet assay was one-way analysis of variance (ANOVA) followed by the Dunnett multiple comparison test. For the CTA assay, experimental data were analysed by Fisher's exact test considering the number of type III foci in the treatments and the surviving cells compared to the corresponding negative control or DMSO solvent control for MCA. Results were considered statistically significant at $P < 0.05$.

Results

Characterisation of ZrO_2 and TiO_2 NP

The experiments were carried out using time, temperature, concentration and medium that closely simulates the experimental conditions used for cellular tests. Table 1 illustrates the results of NP dispersions (sol) state characterisation (pH, Zeta potential and

mean hydrodynamic diameter by intensity) of uncoated, silicated and citrated ZrO_2 NP dispersed in deionised water and complete culture medium, at 0.125 mg/ml. The absorption of BSA of culture medium on powder surfaces is evident. In fact, Z potential assessed for ZrO_2 samples dispersed in deionised water showed different values, according to Z potential-pH curves, while in culture medium negative values were measured for all the samples.

Concerning the hydrodynamic diameters, for the water media the citrate acts as dispersant, producing a diameter decreasing, particularly if added in a low amount. For higher citrate amount, instead, the hydrodynamic diameter increases probably due to the steric effect of the anionic chelant.

Uncoated ZrO_2 in the culture media buffered at pH 7.4 showed a strong aggregation, the hydrodynamic diameter decrease observed over time is consistent with the sample precipitation on the bottom of the cuvette, leaving the smallest particles to float.

In the culture media, the same effect was observed for the low citrated sample, where the citrate added is too poor to change the surface charge and to induce stability changes. Instead, no aggregation was evidenced for the silicated and the high citrated samples, which probably at the buffered pH of 7.4 are more stable and far from their isoelectric points than in deionised water.

TEM imaging of ZrO_2 NP are reported in Figure 1. TEM image of pristine ZrO_2 NP shows a very fine primary nanostructure in accordance with wet chemical sol-gel process employed by manufacturer for the synthesis. Due to higher values of surface energy in comparison with TiO_2 , ZrO_2 nucleation requires higher energy for the formation of stable crystalline nuclei that can grow upper the critical radius. The presence of coating agents did not seem to influence the pristine structure that have an high tendency to form aggregates.

Table 2 illustrates the results of NP dispersions (sol) state characterisation (pH, Zeta potential and mean hydrodynamic diameter by intensity) of uncoated, citrated, silicated TiO_2 NP and Aerioxide®

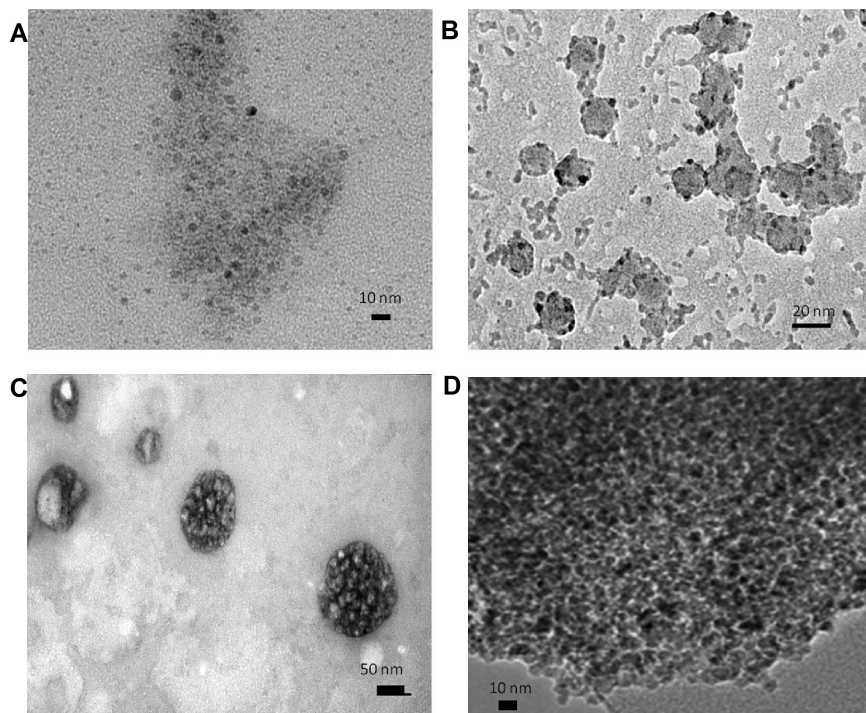


Figure 1. TEM images of ZrO_2 NP. (A) Pristine; (B) silica coated; (C) low-citrate coated; (D) high-citrate coated.

P25 dispersed in deionised water and complete culture medium. Zeta potential of ultrafiltered particles from dispersion in culture medium is also reported, in order to discriminate between contribute of particles and medium components not adsorbed onto particles surface.

Table 2. Mean hydrodynamic size by intensity and Zeta potential for 125 µg/ml of uncoated, citrated, silicated TiO₂ NP and Aerioxide® P25 dispersed in deionized water and complete culture medium

TiO ₂ NP	Deionized water			
	pH	Z-pot (mV)	Mean size (nm)	PdI
Uncoated	2.33	41.2 ± 0.5	83.5 ± 10.4	0.48 ± 0.09
Citratated	5.47	-34.2 ± 1.2	57.5 ± 2.6	0.68 ± 0.05
Silicated	2.84	32.2 ± 4.1	155.6 ± 22.1	0.28 ± 0.01
Aerioxide® P25	4.13	37.4 ± 0.9	489.5 ± 130.5	0.30 ± 0.04
Complete culture medium				
Uncoated				
0 h	7.25	-10.6 ± 1.0	1608 ± 211	1.00 ± 0.01
24 h		-11.4 ± 0.6	1829 ± 99	0.64 ± 0.05
48 h		-10.9 ± 0.6	1962 ± 147	0.98 ± 0.03
72 h		-10.8 ± 0.4	1318 ± 85	0.73 ± 0.22
Ultrafiltered ^a	8.10	-20.9 ± 0.2		
Citratated				
0 h	7.69	-10.7 ± 0.3	68.3 ± 1.2	0.27 ± 0.01
24 h		-10.9 ± 0.2	137.6 ± 0.9	0.21 ± 0.01
48 h		-10.7 ± 0.5	148.6 ± 0.4	0.21 ± 0.01
72 h		-11.6 ± 0.5	157.3 ± 0.4	0.22 ± 0.01
Ultrafiltered ^a	8.20	-20.1 ± 0.8		
Silicated				
0 h	7.56	-10.6 ± 0.4	563.2 ± 84.0	0.80 ± 0.11
24 h		-10.8 ± 0.6	478.6 ± 44.2	0.77 ± 0.15
48 h		-11.0 ± 0.4	619.1 ± 60.1	0.83 ± 0.13
72 h		-11.6 ± 0.7	501.6 ± 81.6	0.89 ± 0.09
Ultrafiltered ^a	8.20	-22.1 ± 0.7		
Aerioxide® P25				
0 h	7.74	-10.2 ± 0.2	477.0 ± 8.1	0.47 ± 0.01
24 h		-11.5 ± 0.4	468.1 ± 16.1	0.43 ± 0.01
48 h		-10.8 ± 0.4	531.6 ± 16.5	0.53 ± 0.11
72 h		-11.5 ± 0.3	489.7 ± 19.8	0.49 ± 0.09

Data are reported as the mean ± standard deviation. PdI, polydispersity index.

^aTiO₂ NP extracted by ultrafiltration from complete culture medium and redispersed in water.

The comparison of sol state characterisation between deionised water and culture medium clearly evidenced the absorption of BSA and more generally of protein components of culture medium on powder surfaces. TiO₂ NP dispersed in water at their natural pH, in fact, showed different values, in accordance with those reported on Z potential versus pH titration curves (Figure 2), with small deviations in absolute Z potential values, due to different concentration of TiO₂ NP used for light scattering and electroacoustic technique.

TiO₂ NP transferred in complete culture medium, due to a buffer effect, meet neutral pH ranging from 7.25 to 7.74 units and showed a slightly negative Z potential, as expected by BSA and other protein components at neutral pH (BSA isoelectric point ≈ 5) (17). In this condition, silicated and citratated TiO₂ NP samples exhibited a good dispersion, whilst uncoated and Aerioxide® P25 dispersions turned instantaneously cloudy. In particular pristine TiO₂ NP partially precipitated, as reflected in the size distribution data obtained which are not readily amenable to interpretation. The observed behaviour is easily explainable by considering that uncoated TiO₂ NP cross the isoelectric point by reversing Z potential sign from positive to negative, with an expected destabilisation of the sample. The same occurred for P25 and silica coated samples, nevertheless the lower increase of hydrodynamic diameter observed is due, in the case of silica to its dispersing ability that prevented a further aggregation, whilst in case of P25 the already aggregated structure in water, revealed by high values of hydrodynamic size, is preserved also in culture medium. Citratated TiO₂ NP did not show any destabilisation effect because maintained a negative Z potential and a good electrostatic stabilisation due to the presence of citrate coating. In order to test if the acid base behaviour shown by all TiO₂ NP samples was due to medium components adsorbed onto their surfaces or to proteins freely dispersed in the medium, samples were ultrafiltered, redispersed in water and Z potential re-measured. The results confirm that all the TiO₂ NP surfaces were coated by proteic components, as explained by the well-known protein corona paradigm (18). Z potential of all ultrafiltered samples was leveled off around -20 mV. In particular, the high deviations shown by uncoated and citratated samples, comparing Z potential in the absence and in the presence of culture medium at pH 8, confirmed the presence of protein coating that masks all TiO₂ NP surfaces. In order to confirm the results, the concentration of BSA was normalised for the surface of TiO₂ samples, as calculated by BET analysis. The results (Table 3) agreed with the formation of BSA coating, being the BSA concentration in all

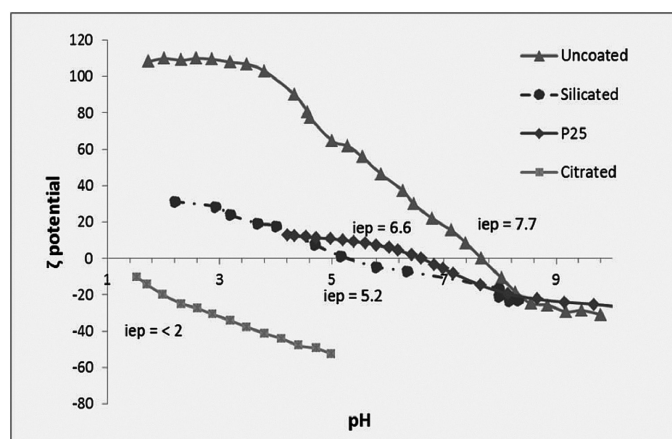


Figure 2. Z Potential versus pH titration curves of TiO₂ NP.

cases higher than the BSA adsorption at the maximum concentration reported in literature, which is about $50\text{ ng}/\text{cm}^2$ (19).

TiO_2 NP TEM imaging are reported in Figure 3. The first evidence arising by comparing different TiO_2 preparation with TiO_2 P25 is the thinner structure of TiO_2 nanosols primary particles (A) as obtained by wet chemical sol-gel process in comparison with P25 that is produced by high temperature flame hydrolysis synthesis (aerosol process, Evonik) (D). Moreover in the silicated sample (B) a homogeneous dispersion of TiO_2 NP (mean diameter $\sim 5\text{ nm}$) within SiO_2 NP (mean diameter $\sim 15\text{ nm}$) can be clearly observed. Finally, in the presence of the organic modifier (C), TiO_2 NP resulted totally embedded in the matrix of citrate, as confirmed by Z potential data.

ZrO_2 and TiO_2 NP internalisation in Balb/3T3 cells

Internalisation results were obtained after Balb/3T3 exposure for 48 h to ZrO_2 and TiO_2 NP.

Cells in complete culture medium (negative control) showed normal morphology of live cells with well-defined nuclei and organelles. The same morphology was observed for most of the cells exposed to NP where no evident signs of toxicity were present. Cells exposed to high citrate coated ZrO_2 (Figure 4H-I), pristine TiO_2 (Figure 5B-D) and citrate coated TiO_2

Table 3. Amount of BSA added, normalized for the TiO_2 NP surface area

	SSA (g/m^2) ^a	ng BSA/ cm^2 TiO_2 ^b
Uncoated TiO_2 NP	154	97
Citrate TiO_2 NP	156	96
Silicate TiO_2 NP	86	174
Aeroxide® P25	60	250

^aSSA, specific surface area determined by BET analysis.

^bAmounts of BSA (ng) adsorbed on TiO_2 NP surface (cm^2).

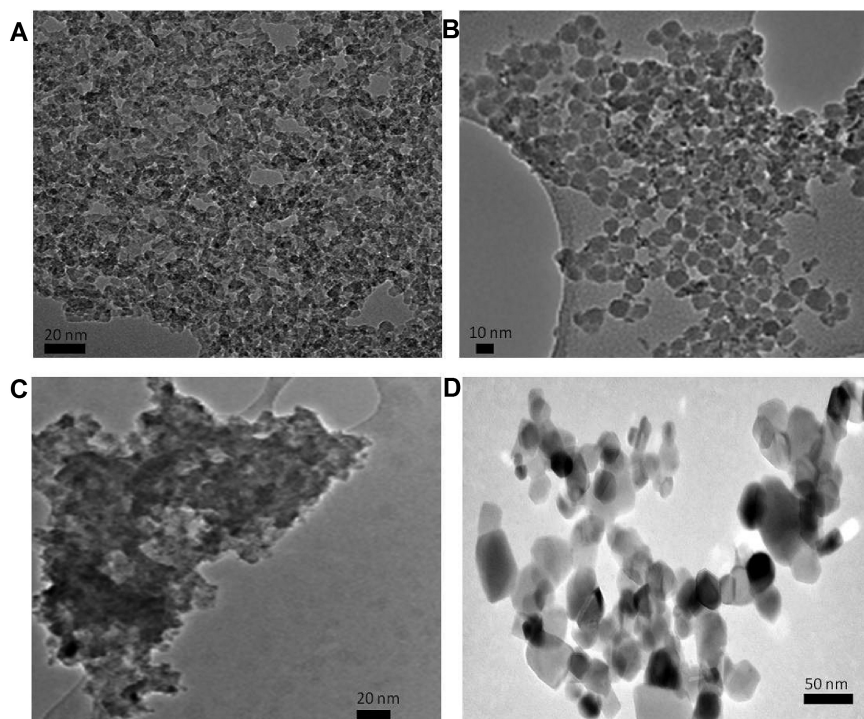


Figure 3. TEM images of TiO_2 NP. (A) pristine; (B) Silica coated; (C) citrate coated; (D) P25.

(Figure 5G-I) showed increasing number of enlarged vacuoles and amorphous material in the cytosol indicating a starting of a possible inflammatory process. However, no apoptosis or cell necrosis was found.

In all the analysed samples, ZrO_2 and TiO_2 NP were observed both inside and outside cells in form of agglomerates/aggregates.

A possible mechanism of phage-endocytosis with autophagic lysosome transport and release of NP in the cytosol was observed in each sample. Lamellar bodies, probably involved in secretory process, were found after exposure to P25 (Figure 5K-L).

Cell viability

As shown in Figure 6, ZrO_2 NP did not affect the Balb/3T3 viability cells after 24, 48 and 72 h of exposure. After 24 h treatment, only the lowest dose of low citrated ZrO_2 NP showed a statistical significant effect ($P < 0.05$), however as the effect falls in the sub-toxic range, the result can be considered due to biological variability. After 72 h, only the higher dose of pristine ZrO_2 NP showed a statistical significant effect ($P < 0.05$).

Figure 7 shows the dose-response curves for TiO_2 NP after 24, 48 and 72 h of exposure. The data obtained showed that all NP induced a cytotoxic effect in Balb/3T3 starting from a time of exposure of 24 h.

Cytostasis and cell death

Cytostasis was measured by CBPI and RI, and cell death by apoptotic and necrotic indices. CBPI and RI showed a cytostatic effect for both pristine and remediated ZrO_2 NP on Balb/3T3 cells compared to the untreated control (Figure 8). TiO_2 NP induced a mild effect (Figure 9). Only the higher doses of pristine TiO_2 , 10 and 20 $\mu\text{g}/\text{cm}^2$ of citrated and 20 $\mu\text{g}/\text{cm}^2$ of P25 induced a statistically significant effect. The same effects were observed by the RI.

The apoptotic and necrotic indices showed that all ZrO_2 NP were cytotoxic to Balb/3T3 (Figure 8). Regarding TiO_2 NP apoptotic cells were induced by citrated NP and by P25, while necrotic cells were induced by all the NP tested (Figure 9).

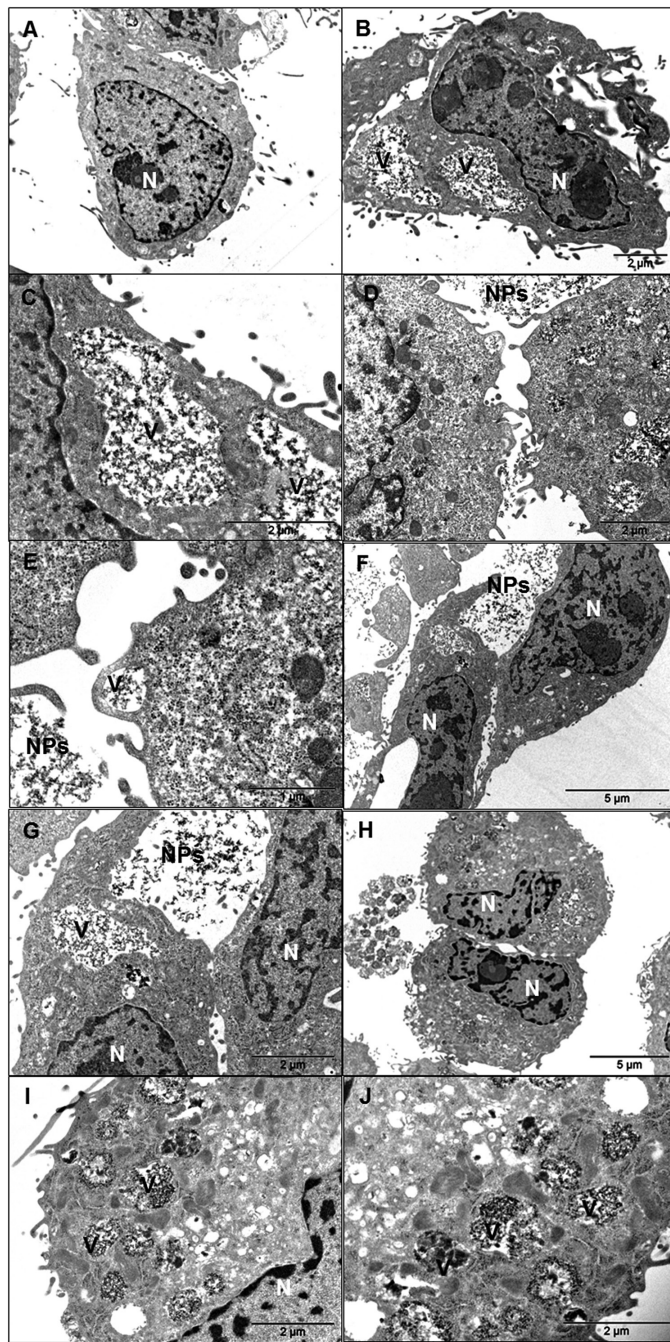


Figure 4. TEM images of Balb/3T3 cells cultured for 48h in complete cell culture medium (**A**, negative control) and exposed for 48h to 20 $\mu\text{g}/\text{cm}^2$ of: pristine ZrO_2 (**B**, **C** magnification of B); silicated ZrO_2 (**D**, **E** = magnification of D); low-citriated ZrO_2 (**F**, **G** = magnification of F); high-citriated ZrO_2 (**H**, **I**, **J** = increasing magnifications). N: nucleus; V: vesicles with NP inside; NP, nanoparticles.

Chromosomal damage

As shown in Figure 10, the highest doses of pristine, silicate coated and high citrate coated as well as the 10 $\mu\text{g}/\text{cm}^2$ dose of high citrate coated ZrO_2 NP, significantly induced micronuclei formation. NPB were induced by all the tested doses of the pristine ZrO_2 NP and by the 10 and 20 $\mu\text{g}/\text{cm}^2$ of the low citrated coated NP. NBUD formation was induced in a statistically significant manner only following exposure with the higher dose of pristine ZrO_2 NP (Figure 10).

Also TiO_2 NP induced a mild formation of micronuclei respect to negative control. Only the citrated TiO_2 NP and the lowest tested concentration of P25 induced a statistically significant formation of micronuclei (Figure 11). TiO_2 NP exposure did not increase the NPB

frequency (Figure 11). Similarly many of the experimental conditions tested did not induce NBUD formation (Figure 11), except for the 40 $\mu\text{g}/\text{cm}^2$ citrated and 10 $\mu\text{g}/\text{cm}^2$ of Aerioxide® P25, which enhanced significantly NBUD frequency.

Comet assay

Following 2h treatment, each concentration of all the tested ZrO_2 NP induced a significant increase of primary DNA damage in Balb/3T3 (Figure 12). After 24h of treatment quite all the tested concentrations induced an increase of DNA fragmentation, although to a lesser extent (Figure 12). Following 48 and 72h of exposure, there is a reduction of the DNA damage exerted by ZrO_2 NP.

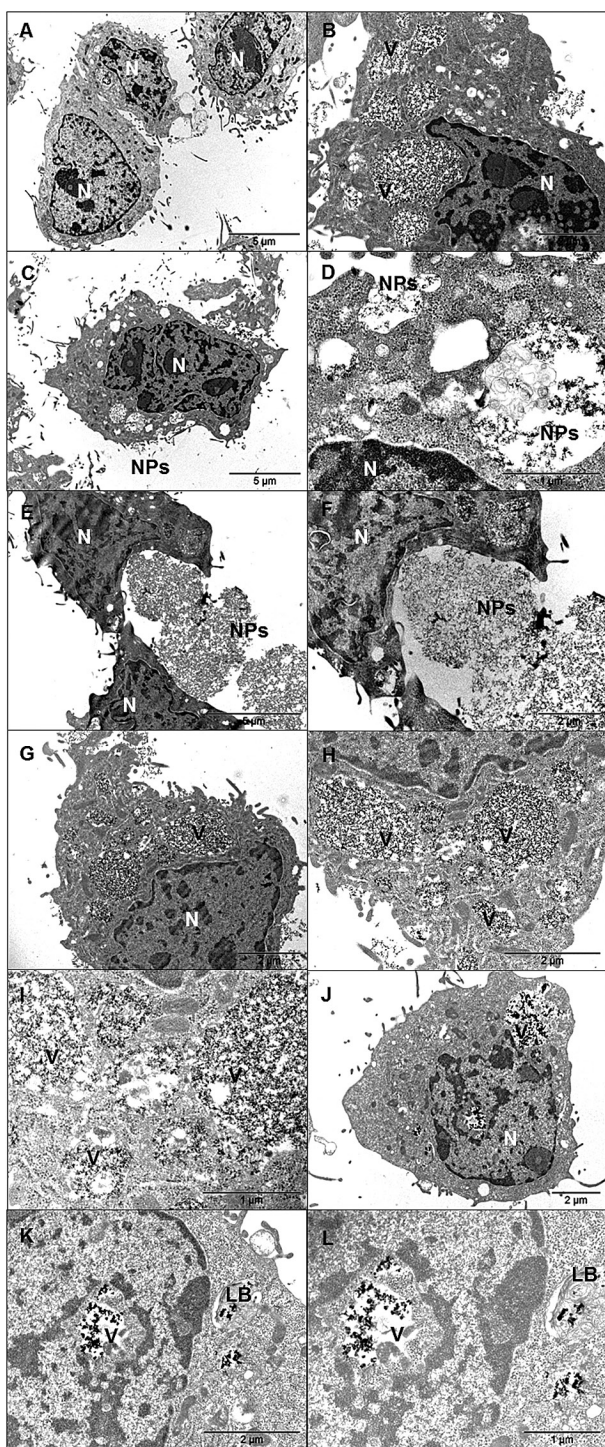


Figure 5. TEM images of Balb/3T3 cells cultured for 48 h in complete cell culture medium (**A**, negative control) and exposed for 48 h to $20 \mu\text{g}/\text{cm}^2$ of: pristine TiO_2 (**B–D** = magnification of **C**); silicate TiO_2 (**E**, **F** = magnification of **E**); citrated TiO_2 (**G–I** = increasing magnifications); P25 (**J–L** = increasing magnifications). N: nucleus; V: vesicles with NP inside; NP, nanoparticles; LB, lamellar bodies.

Oxidative comet assay showed that only the lower concentration of pristine ZrO_2 NP induced a statistically significant effect after 2 h, while following 24 h of exposure only 20 and $40 \mu\text{g}/\text{cm}^2$ of the silica coated ones slightly increased oxidised pyrimidines, Endo-III sensitive sites (Figure 13). Oxidation of purines, Fpg sensitive sites,

increased significantly at all the tested concentrations of silica-coated ZrO_2 NP at 2 h treatment, but this effect was lost after 24 h of treatment. The low citrate-coated NP induced a significant effect only at the highest concentration (2 h treatment), and at $20 \mu\text{g}/\text{cm}^2$ after 24 h of exposure (Figure 13).

The genotoxicity exerted by TiO_2 in Balb/3T3 cells investigated by comet assay showed that after both 2 and 24 h treatment all the NP induced a significant increase of primary DNA damage while, as shown for ZrO_2 NP, after 48 and 72 h the level of DNA damaged was very low (Figure 14).

Both oxidised pyrimidines and purines increased significantly at quite all the tested concentrations of TiO_2 NP as compared to baseline values, following the 2 and 24 h of treatment (Figure 15).

Morphological neoplastic transforming potential

As shown in Figure 16A, the pristine and both low and high citrate coated ZrO_2 NP induced statistically significant morphological transformation in Balb/3T3 cells at all the tested concentrations.

Regarding TiO_2 NP, only the citrate coated and the P25 induced type-III foci in Balb/3T3 cells (Figure 16B).

Discussion

In this study internalisation analysis showed that both ZrO_2 and TiO_2 NP were localised both inside and outside of the Balb/3T3 cells in form of agglomerates/aggregates after 48 h of treatment at a concentration of $20 \mu\text{g}/\text{cm}^2$ (Figures 4 and 5). The majority of the cells exposed to NP did not show signs of toxicity. However the high-citrate coated ZrO_2 NP and pristine and citrate coated TiO_2 NP induced increasing number of enlarged vacuoles and amorphous material in the cytosol, likely indicating the beginning of a possible inflammatory process, however without signs of cell death as increase of apoptotic or necrotic cells was not found.

CFE assay showed that ZrO_2 NP did not affect Balb/3T3 clonogenicity. On the other hand, by scoring the apoptotic and necrotic cells, we observed that ZrO_2 NP were able to induce cell death. Furthermore CBPI and RI indices were significantly lower in cells treated with ZrO_2 NP respect to the negative control.

Starting by a treatment of 24 h, CFE showed that TiO_2 NP were able to induce cytotoxic effects. From the results of CBMN-cyt assay, it is evident that only the citrated titania and P25 were able to exert apoptosis while all NP were able to induce necrosis, although only the P25 at all the tested doses. Cytostatic effects were induced only by the pristine, the citrated NP and by the P25.

This apparent discordance regarding the cytotoxicity results obtained with the CFE test and cytome assay, in particular regarding ZrO_2 NP, could be due to the fact that these assays measure cell proliferation by taking into account distinct endpoints and by using different experimental designs. In fact the cytome assay measures the frequency of cell division and the evaluation occurs directly after the end of the NP exposure. On the contrary, the CFE assay does not refer to a specific mechanism of cytotoxicity, and colonies can originate from any surviving cell following 7 days of culture and after 4 days by the end of the exposure period (20). Taken together these data suggest that ZrO_2 NP are able to induce cell death, however cells not too heavily damaged remain viable, continue to replicate themselves and are able to form colonies. Hence ZrO_2 NP, in our experimental design, do not seem to possess a strong cytotoxic property and this is in agreement with literature data. In fact some studies reported no capacity by ZrO_2 NP to induce cytotoxic effects (21–23) and only few studies reported a moderate cytotoxic potential (24,25).

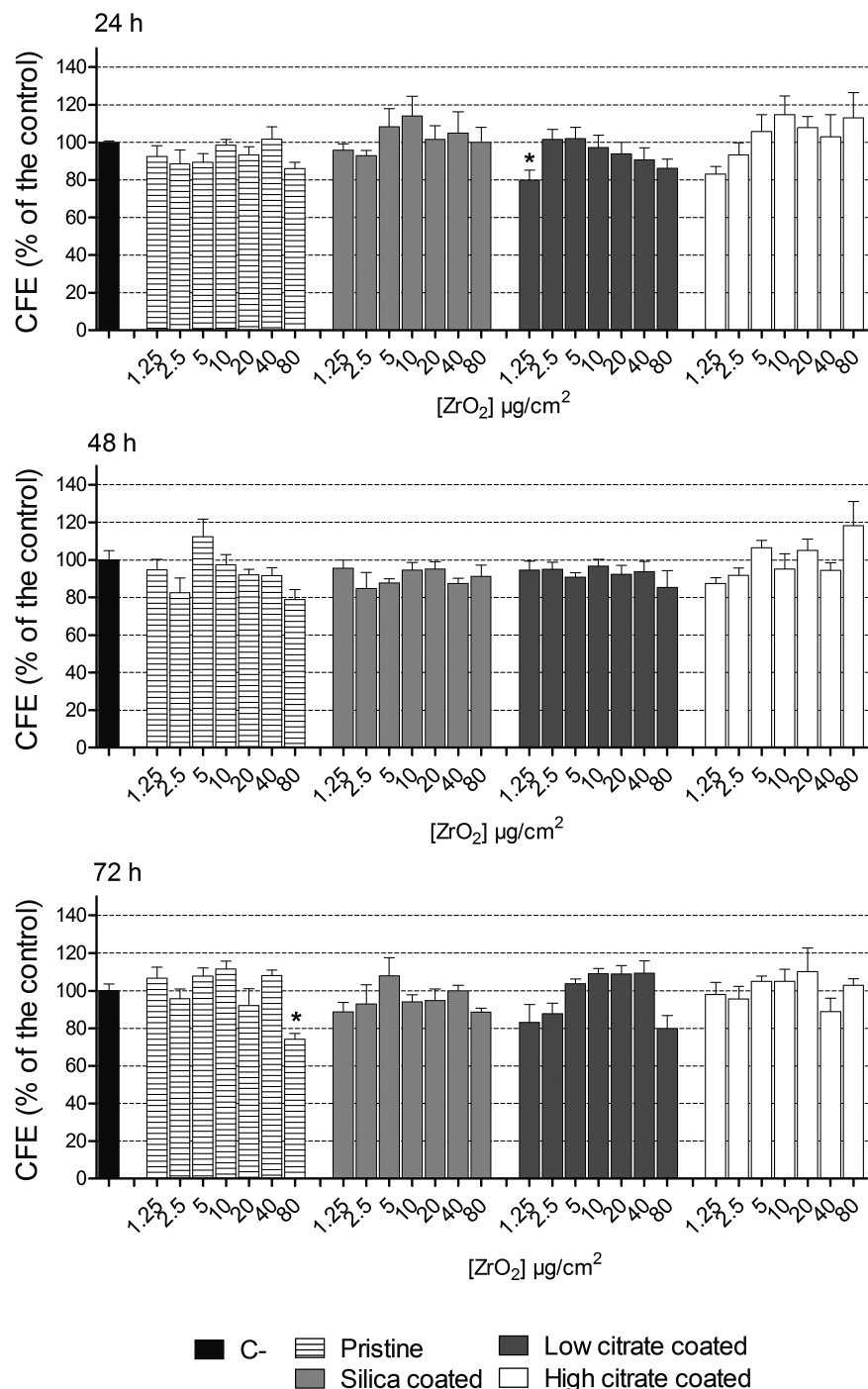


Figure 6. Cell viability in Balb/3T3 cells exposed to ZrO₂ NP evaluated by CFE assay. Cells were exposed to increasing concentrations (1.25–80 μg/cm²) of NP for 24, 48 and 72 h. Data are plotted as mean %CFE values normalized to the untreated control (C-; black bar) ± standard error of the mean (SEM); *n* = 6. *P < 0.05, **P < 0.01, ***P < 0.001. C+: 1 μM Na₂CrO₄ that induced 0% CFE (data not shown).

The effects of TiO₂ NP on cell viability are reported by several studies available in the literature. Regarding the toxic effects of anatase TiO₂ NP, the crystalline form used in this study, literature results are conflicting. Cytotoxic potential of TiO₂ NP was observed in human bronchial epithelial BEAS-2B cells (26), in IMR90 human bronchial fibroblasts cells (27), in human umbilical vein endothelial cells (28), in rat and human glial cells (29) and in Syrian Hamster Embryo Cells (SHE cells) where an EC₅₀ value at the dose of 10 μg/cm² was obtained (30). However some researchers failed to find

cytotoxic potential of anatase TiO₂ NP in human peripheral blood lymphocytes (PBL) (31), in human hepatoma HepG2 cells (32) and in A549 human lung carcinoma cells (33). Obviously possible variability source in the results reported in literature may derive by the different cell type employed, the presence of serum, different characteristics of NP and the tested doses. Another point to take into account is the ability of NP to interfere with the classical colorimetric tests used for the study of cytotoxicity, such as WST-1, MTT or Neutral Red (34,35). In this context, CFE is an *in vitro* method for

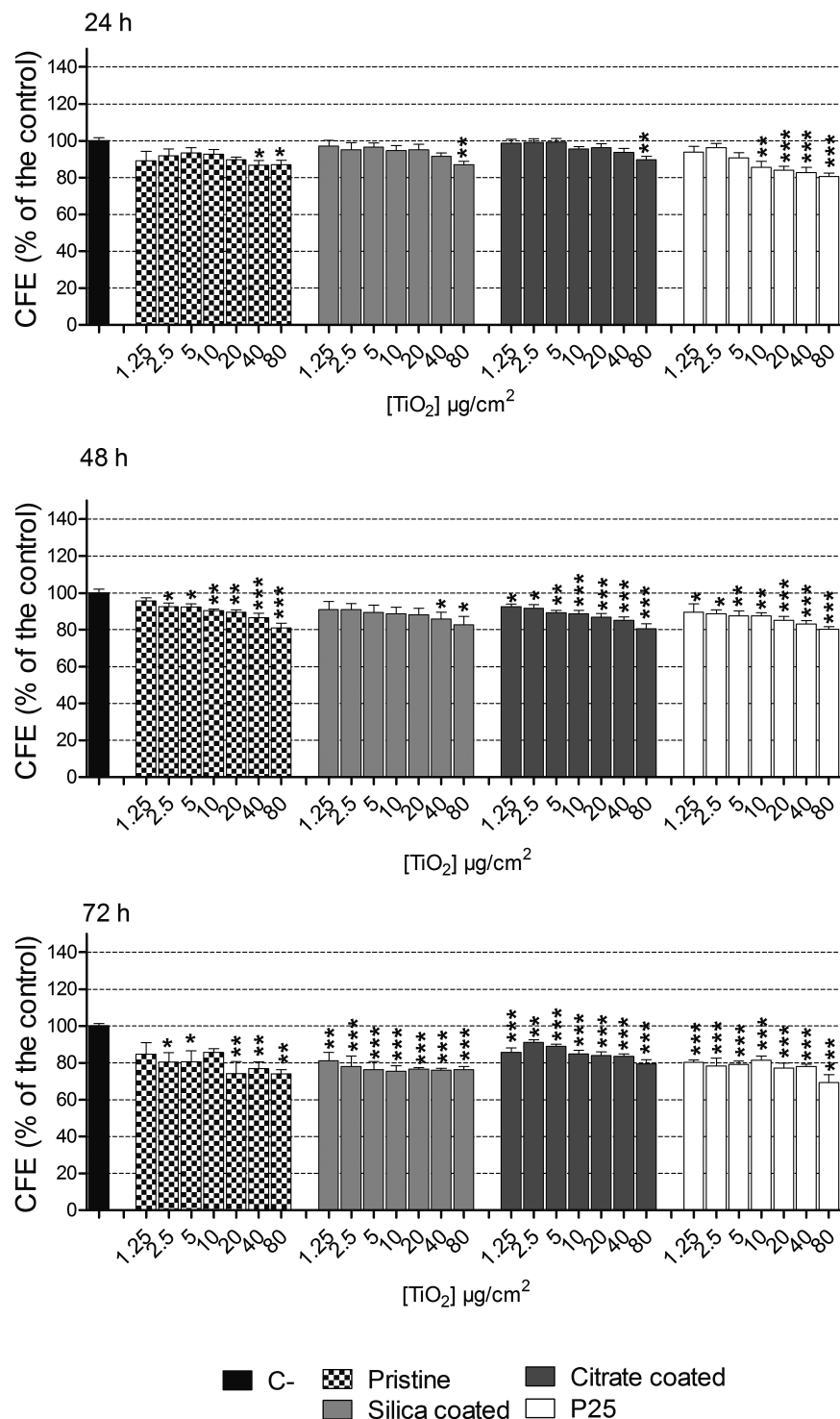


Figure 7. Cell viability in Balb/3T3 cells exposed to TiO_2 NP evaluated by CFE assay. Cells were exposed to increasing concentrations ($1.25\text{--}80\text{ }\mu g/cm^2$) of NP for 24, 48 and 72 h. Data are plotted as mean %CFE values normalized to the untreated control (C-; black bar) \pm standard error of the mean (SEM); $n = 6$. * $P < 0.05$, ** $P < 0.01$, *** $P < 0.001$. C+: 1 μM Na_2CrO_4 that induced 0% CFE (data not shown).

the assessment of basal cytotoxicity which is noncolorimetric and nonfluorescent, avoiding thus possible interferences of NP with the toxicity assessment. In this context the European Commission's Joint Research Centre (JRC) coordinated an interlaboratory comparison study on CFE for assessing the cytotoxicity of NP and the results obtained showed that CFE assay is a suitable and robust *in vitro* method to assess cytotoxicity of NP (36).

Genotoxicity evaluated by means of MN frequency demonstrated that ZrO_2 and TiO_2 NP possess a low capacity to induce micronuclei. Our data are in agreement with previous studies in SHE cells (30) and in A549 cells (33) treated with pristine TiO_2 NP. However some researchers found that TiO_2 NP induced micronuclei formation in PBL (37) and in human epithelial cells (38). In human embryonic kidney (HEK293) and NIH/3T3 cells a statistically significant

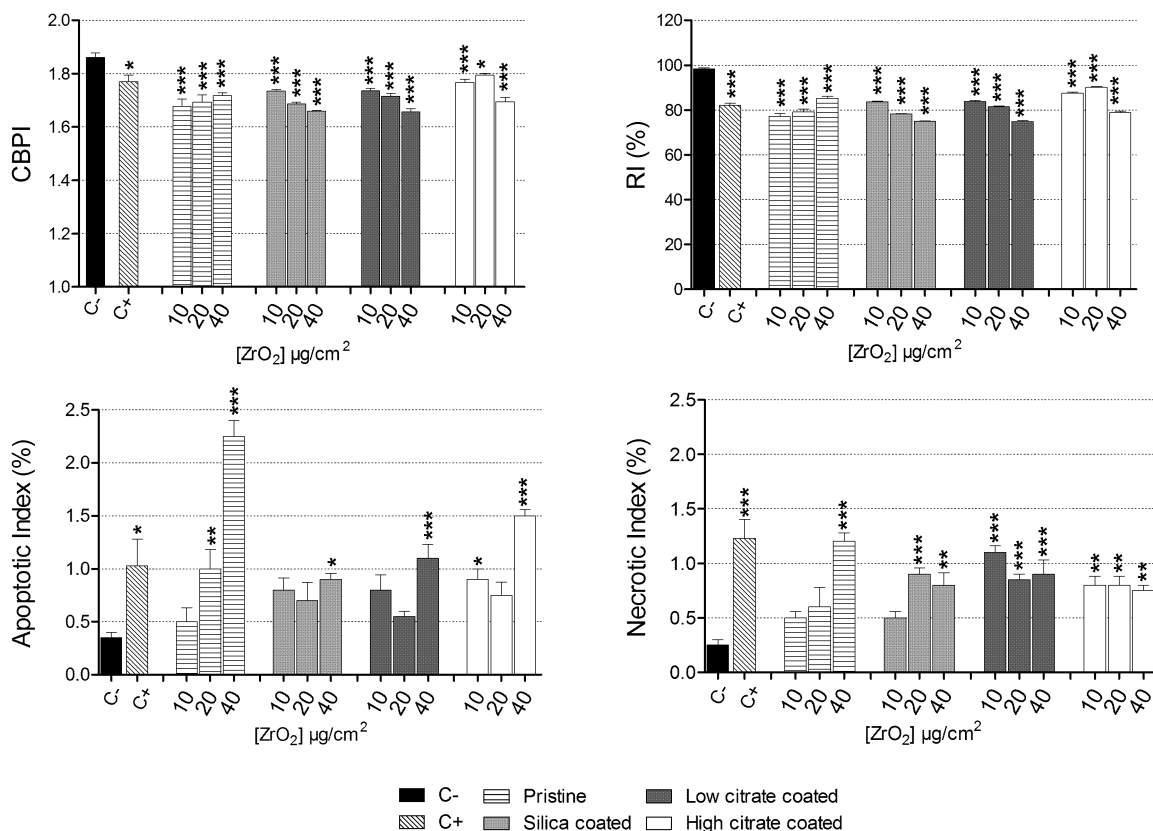


Figure 8. Cytostatic (CBPI and RI) and cytotoxic (apoptotic and necrotic index) effects induced by ZrO_2 NP. Cells were exposed to increasing concentrations ($10-40 \mu\text{g}/\text{cm}^2$) of NP for 48 h. Data are plotted as mean values \pm standard error of the mean (SEM); $n = 4$. * $P < 0.05$, ** $P < 0.01$, *** $P < 0.001$. As positive control 0.10 $\mu\text{g}/\text{ml}$ mitomycin-C was employed.

induction of micronuclei was observed when cells were exposed to 1000 $\mu\text{g}/\text{ml}$ (a concentration much higher than that used in our study) of two anatase NP (39). One of the factors that could contribute to the differences observed in those studies is that the induction of micronuclei by TiO_2 NP is affected by the characteristics of the culture medium including its capacity to decrease the agglomeration and to increase the NP-cell interaction (39,40). It is also evident from some studies that the formation of micronuclei is correlated to the size of the NP; for example, it was observed an increased MN frequency after exposure of SHE cells to TiO_2 NP of 20 nm, but not of 200 nm (41) as well as in BEAS-2B cells exposed to TiO_2 NP of 10 and 200 nm, but not to TiO_2 NP > 200 nm (42).

To the best of our knowledge, there is no available literature concerning micronuclei induction by ZrO_2 NP.

Comet assay revealed that after 2 h exposure all the tested ZrO_2 NP at all the doses were able to induce DNA damage, and after 24 h only the higher doses of the pristine, low-citrate and high citrate-coated NP did not induce significant effects. On the other hand after 48 and 72 h of exposure, minor DNA damage was found. Similar results were observed for TiO_2 NP. For this reason, we decided to apply the modified protocol of comet assay to determine the presence of oxidised pyrimidine and purine bases in cells exposed for 2 and 24 h to NP. Inclusion of EndoIII enzyme in the protocol revealed that only pristine and silica-coated ZrO_2 NP were able to induce oxidation of pyrimidines while oxidation of purines was induced by silica-coated and low citrate-coated ZrO_2 NP. On the other hand, all TiO_2 NP were able to induce both pyrimidine and purine oxidation.

Only few studies investigated the genotoxic potential of ZrO_2 NP. In PBL and cultured human embryonic kidney (HEK293) cells, exposure to ZrO_2 NP did not induce significant primary and oxidative DNA damage (22). In an *in vivo* study, ZrO_2 NP did not show genotoxic potential in the wing spot assay of *Drosophila melanogaster* (43). Conflicting results about the capacity of anatase TiO_2 NP to induce primary and oxidative DNA damage are reported. Positive results were obtained in HepG2 cells (32), in HEK293 and NIH/3T3 cell lines (39), and in SHE cells (30). Negative results were observed in IMR 90 and BEAS-2B cells (27), in cells of the human nasal mucosa and in PBL (31,44). Jugan and collaborators observed that TiO_2 NP of 12 and 142 nm induced DNA strand breaks after 4 h of exposure in A549 cells and that after 24 h only the 12 nm sized NP induced DNA damage, while after 48 h the frequency of breaks drastically decreased in exposed cells (33). The results of the study by Jugan and collaborators are similar to our results that show the capacity of comet assay to detect DNA strand breaks is strictly dependent on the time of exposure, and that shorter is the time of exposure, higher is the damaged DNA detectable, likely due to the fact that cells have not enough time to repair most of the damage induced. Other factors could explain the time-related genotoxic effects of NP observed with comet assay such as an adaptive response of the cells or a dilution effect of NP following cell replications (45).

Carcinogenic potential of ZrO_2 and TiO_2 NP was evaluated by CTA assay, an *in vitro* test that has attracted attention within the field of alternative methods due to its potential to reduce the number of animals sacrificed to assay carcinogenicity *in vivo* (46).

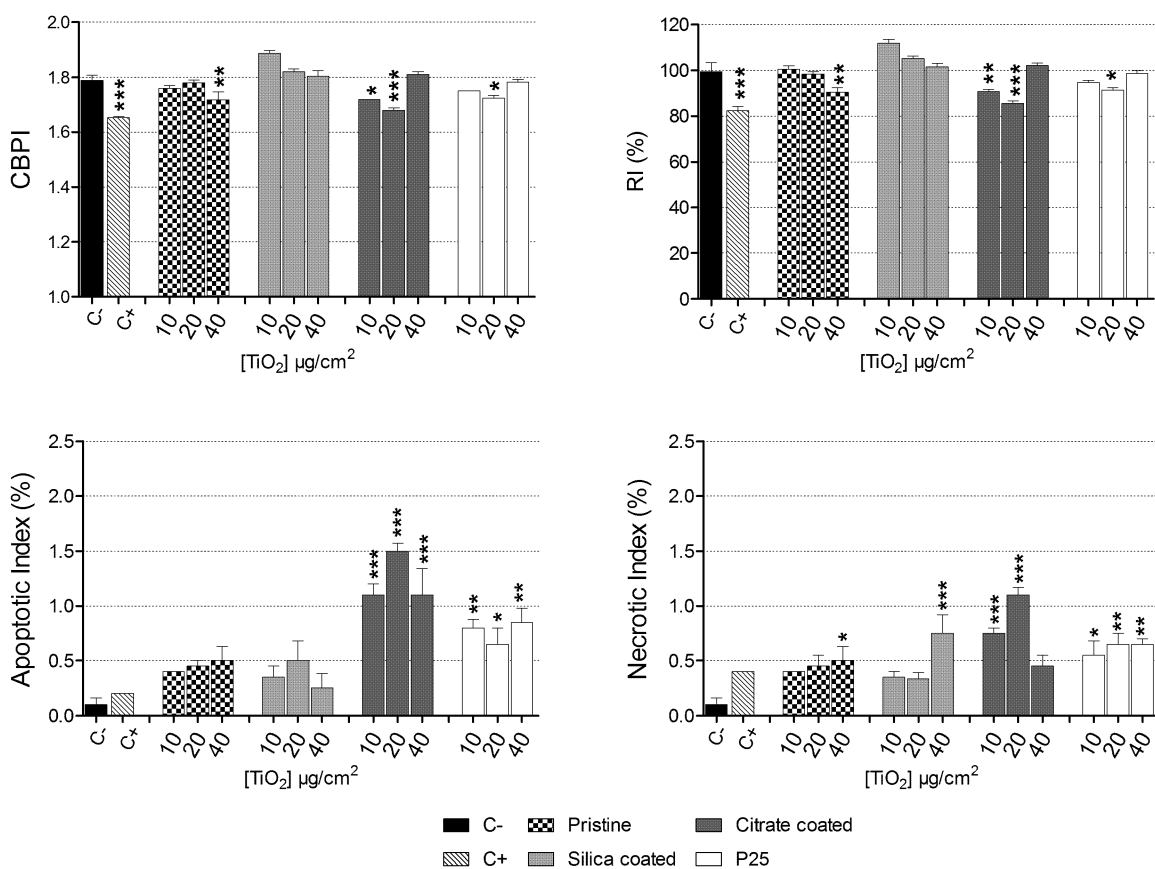


Figure 9. Cytostatic (CBPI and RI) and cytotoxic (apoptotic and necrotic index) effects induced by TiO_2 NP. Cells were exposed to increasing concentrations ($10-40 \mu g/cm^2$) of NP for 48h. Data are plotted as mean values \pm standard error of the mean (SEM); $n = 4$. * $P < 0.05$, ** $P < 0.01$, *** $P < 0.001$. As positive control, 0.10 $\mu g/ml$ mitomycin-C was employed.

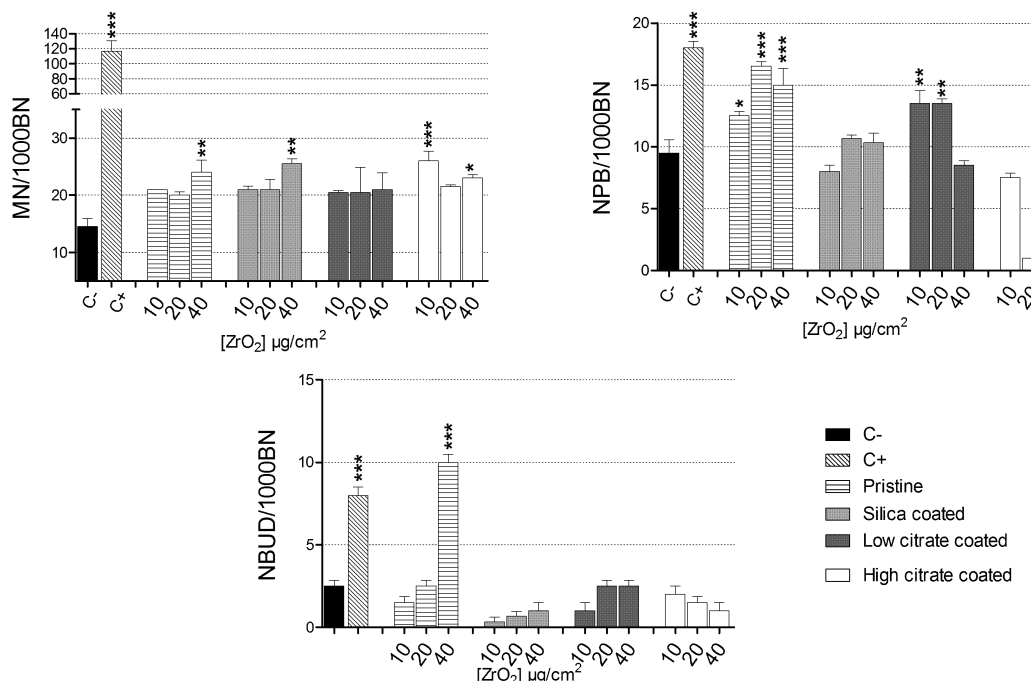


Figure 10. Chromosomal damage induced by ZrO_2 NP. Balb/3T3 cells were exposed to $10-40 \mu g/cm^2$ NP for 48h and micronuclei, NPB and NBUD were manually scored using an inverted microscope (400 \times magnification). Data are plotted as mean values \pm SEM; $n = 4$; statistical analysis performed by one-way ANOVA and Dunnett post-test. * $P < 0.05$, ** $P < 0.01$, *** $P < 0.001$. As positive control 0.10 $\mu g/ml$ mitomycin-C was employed.

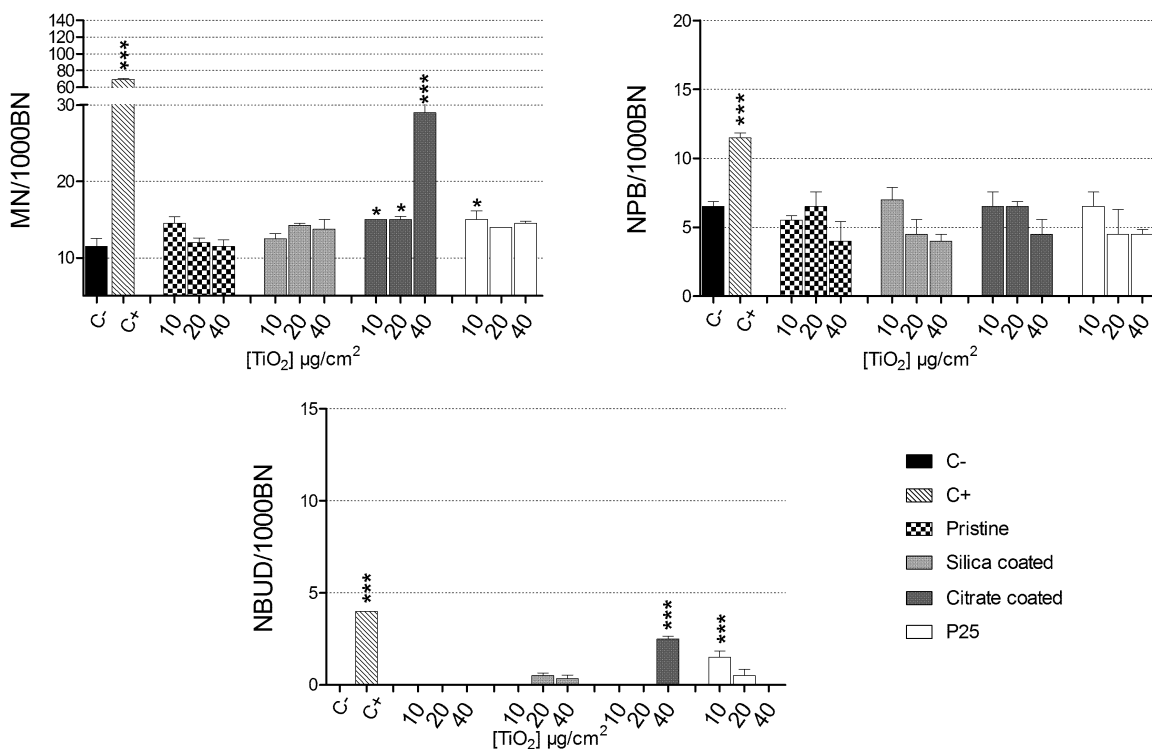


Figure 11. Chromosomal damage induced by TiO_2 NP. Balb/3T3 cells were exposed to 10–40 $\mu\text{g}/\text{cm}^2$ NP for 48h and micronuclei, NPB and NBUD were manually scored using an inverted microscope (400 \times magnification). Data are plotted as mean values \pm SEM; $n = 4$; statistical analysis performed by one-way ANOVA and Dunnet post-test. * $P < 0.05$, ** $P < 0.01$, *** $P < 0.001$. As positive control 0.10 $\mu\text{g}/\text{ml}$ mitomycin-C was employed.

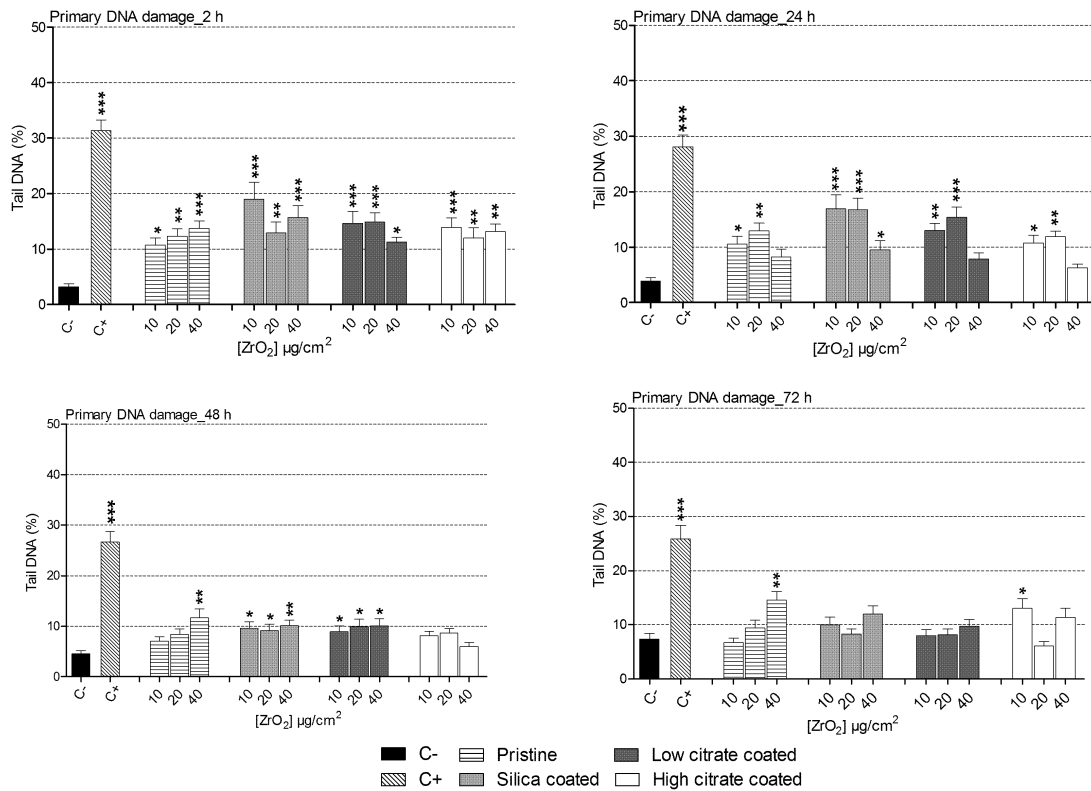


Figure 12. Primary DNA damage induced by ZrO_2 NP. Balb/3T3 were treated with increasing concentrations (10–40 $\mu\text{g}/\text{cm}^2$) of NP for 2, 24, 48 and 72 h. Each data point represents the mean \pm SEM of two independent experiments. C+: positive control (50 μM H_2O_2); C-: untreated control. Statistical analysis performed by one-way ANOVA and Dunnet post-test. * $P < 0.05$; ** $P < 0.01$; *** $P < 0.001$.

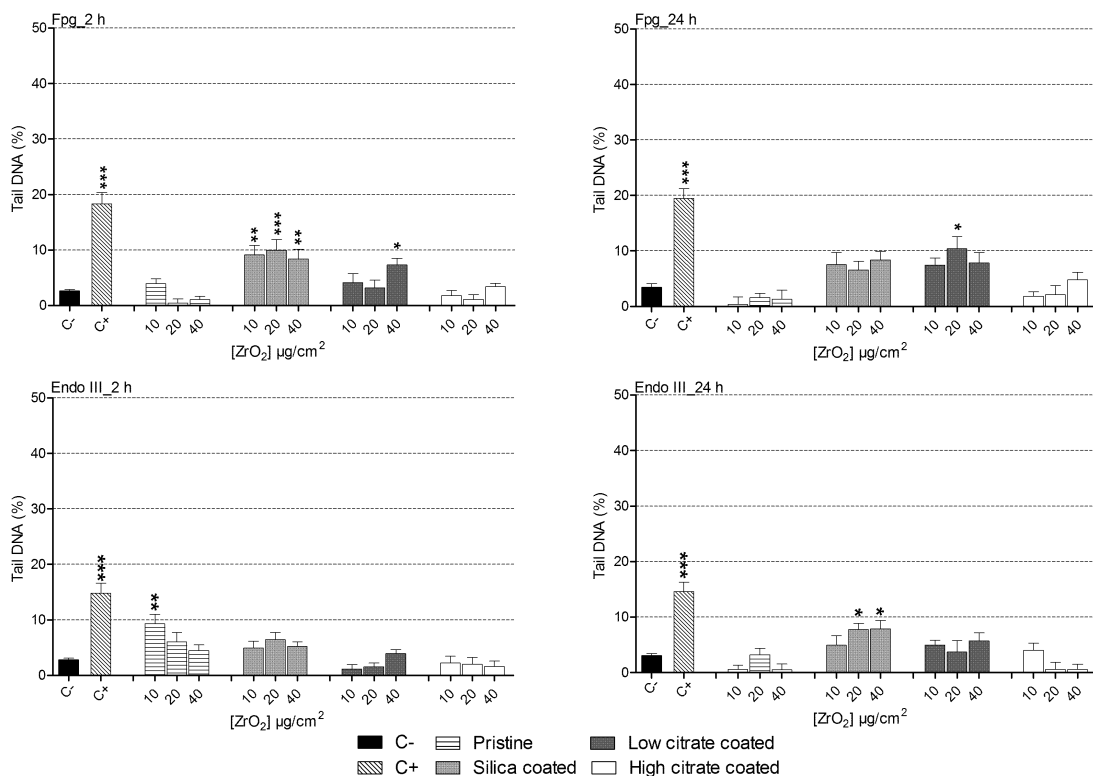


Figure 13. Oxidised DNA lesions induced by ZrO_2 NP. Balb/3T3 were treated with increasing concentrations (10–40 $\mu\text{g}/\text{cm}^2$) of NP for 2 and 24 h. The level of enzyme-sensitive sites was obtained by subtracting the value of % of DNA fluorescence in tail obtained after digestion with each enzyme and with the buffer only. Each data point represents the mean \pm SEM of two independent experiments. C+: positive control (50 μM H_2O_2); C-: untreated control. Statistical analysis performed by one-way ANOVA and Dunnett post-test. * $P < 0.05$; ** $P < 0.01$; *** $P < 0.001$.

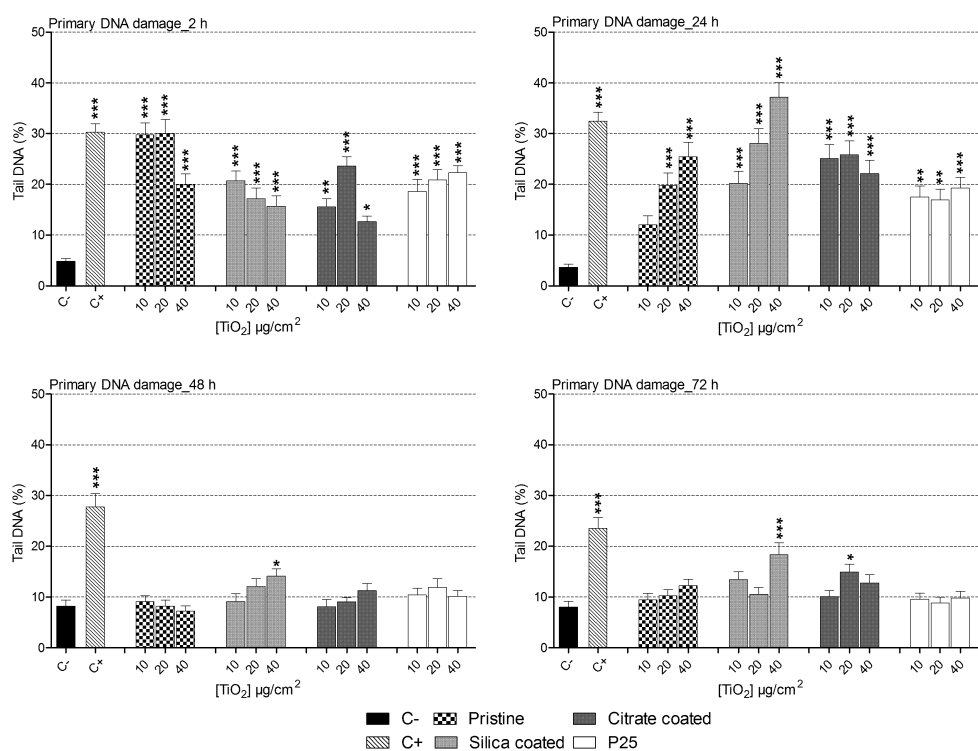


Figure 14. Primary DNA damage induced by TiO_2 NP. Balb/3T3 were treated with increasing concentrations (10–40 $\mu\text{g}/\text{cm}^2$) of NP for 2, 24, 48 and 72 h. Each data point represents the mean \pm SEM of two independent experiments. C+: positive control (50 μM H_2O_2); C-: untreated control. Statistical analysis performed by one-way ANOVA and Dunnett post-test. * $P < 0.05$; ** $P < 0.01$; *** $P < 0.001$.

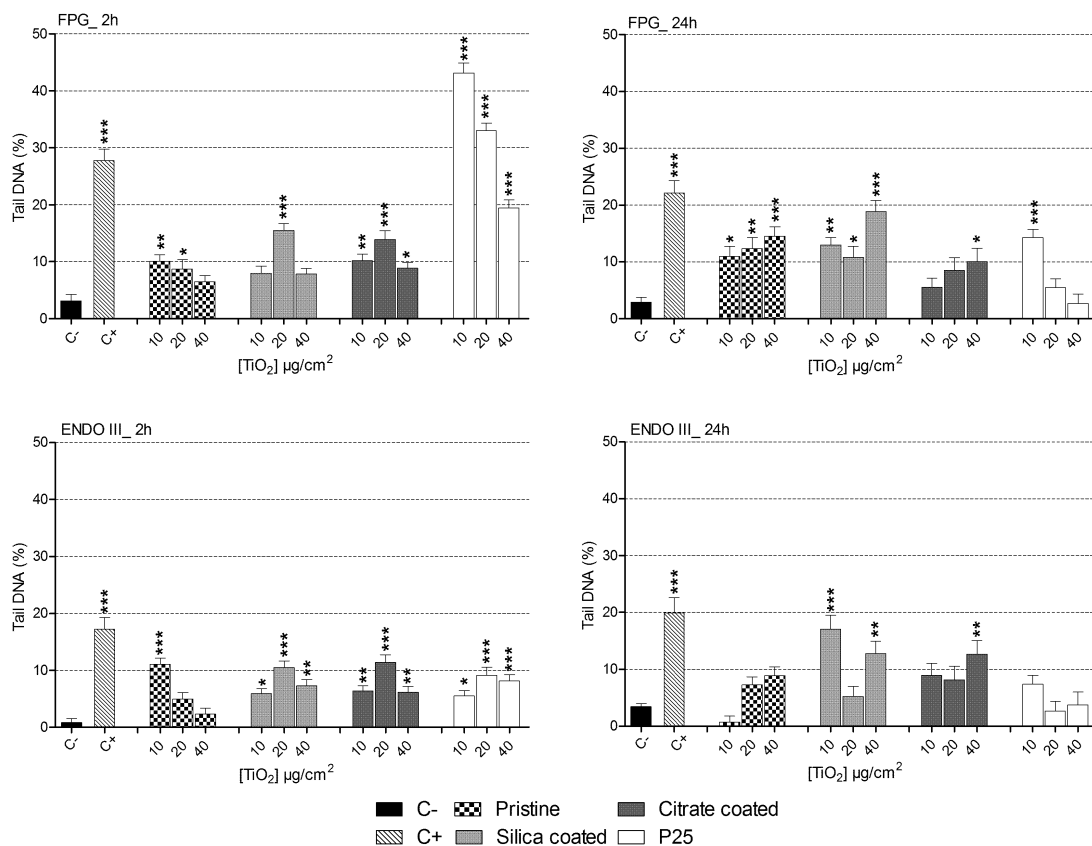


Figure 15. Oxidised DNA lesions induced by TiO_2 NP. Balb/3T3 were treated with increasing concentrations ($10-40 \mu\text{g}/\text{cm}^2$) of NP for 2 and 24h. The level of enzyme-sensitive sites was obtained by subtracting the value of % of DNA fluorescence in tail obtained after digestion with each enzyme and with the buffer only. Each data point represents the mean \pm SEM of two independent experiments. C+: positive control ($50 \mu\text{M H}_2\text{O}_2$); C-: untreated control. Statistical analysis performed by one-way ANOVA and Dunnett post-test. * $P < 0.05$; ** $P < 0.01$; *** $P < 0.001$.

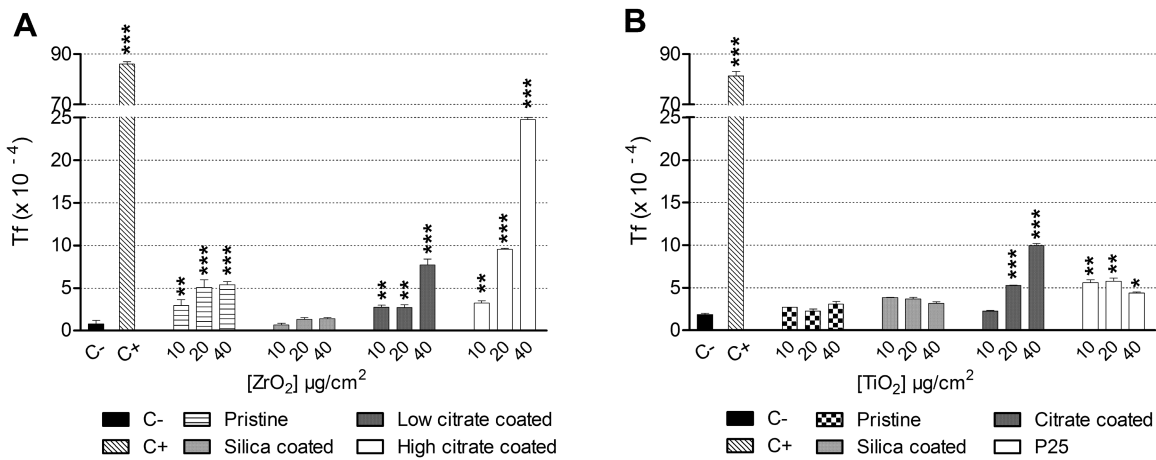


Figure 16. ZrO_2 (A) and TiO_2 (B) NP CTA results. Balb/3T3 cells were exposed for 72h to increasing concentrations of NP. To evaluate the carcinogenicity of ZrO_2 NP, the transformation frequency was calculated and data were compared to the untreated control cells (C-). The statistical significance was evaluated by Fisher exact test in respect to untreated control. Data are presented as mean values \pm SEM; $n = 3$; * $P < 0.05$, ** $P < 0.01$, *** $P < 0.001$. C+: 3 $\mu\text{g}/\text{ml}$ methylcholanthrene.

Regarding ZrO_2 NP, only the silica-coated form did not induce transformation of Balb/3T3 suggesting that the presence of silica coating is able to protect Balb/3T3 from the formation of type-III foci and therefore from morphological transformation. These results are consistent with a previous publication which reported that SiO_2 NP did not induce the formation of type III foci in Balb/3T3 cells (14). Moreover high performance zirconia toughened alumina

(ZTA) materials did not induce DNA damage, mutagenicity and carcinogenicity in C3H/10T_{1/2} mouse fibroblasts (47) and zirconia polycrystals did not elicit mutagenic or transforming effects on irradiated C3H/10T_{1/2} cells (48).

CTA results on TiO_2 NP showed that pristine and silica-coated NP did not induce cell transformation, but both citrate coated and P25 induced the formation of type III foci. To date, the current

Table 4. Summary of results obtained with NP tested with comparable doses and time treatment

Endpoint	ZrO_2 pristine	ZrO_2 silica coated	ZrO_2 low citrate coated	ZrO_2 high citrate coated	TiO_2 pristine	TiO_2 silicate coated	TiO_2 citrate coated	Aeroxide P25
CFE	–	–	–	–	+	–	+	+
Cytostasis	+	+	+	+	+	–	–	–
Apoptosis	+	+	+	+	–	–	+	+
Necrosis	+	+	+	+	+	+	–	+
Micronuclei, NBUD and NPB	+	+	–	+	–	–	+	–
Primary Comet Assay	–	+	–	–	+	+	–	+
Endo III	–	+	–	–	–	+	+	–
Fpg	–	+	–	–	+	+	+	–
CTA	+	–	+	+	–	–	–	+

+ indicates statistically significant effect respect to the negative control; – indicates no statistically significant effect with respect to the negative control.

literature about TiO_2 , that in 2010 has been recognised as a possible carcinogen for humans (group 2B, 49), does not present studies on the carcinogenic potential of TiO_2 NP tested by CTA. However, the ability to induce cell transformation in human embryonic kidney (HEK293) and in mouse embryonic fibroblast (NIH/3T3) cells exposed to TiO_2 NP for 3 weeks was shown (40). Also in BEAS-2B cells treated for up to 4 weeks with TiO_2 a significant increase in the number of clones growing in an anchorage-independent way were observed (50). Changes in cell morphology, enhanced cell proliferation and growth on soft agar, accompanied with increased chromosomal instability, in NIH-3T3 cells after 12 weeks of exposure were also observed (51).

As discussed above, according to our findings the remediation of ZrO_2 and TiO_2 NP has not proven effective in modifying cyto- and genotoxic properties of the tested nanomaterials. Regarding CTA results, only the presence of silica coating has been effective in preventing the type III foci formation of pristine ZrO_2 NP, possibly making safer the nanomaterial. On the other hand, both TiO_2 and ZrO_2 NP coated with citrate induced a strong transforming effect. These results are indicative that citrate itself could possess genotoxic and cell transforming properties. In this regard, Huk and collaborators (52) coated silver NP (Ag NP) with trisodium citrate in order to provide a negative charge on NP. They observed that the coated NP induced HPRT gene mutations in V79-4 cells, and that either sodium citrate alone was able to induce mutations analogously to those induced by Ag NP coated with citrate. Regarding remediated NP investigated in current study, in literature are reported only toxic effects of silica coated TiO_2 NP showing conflicting results. In an *in vivo* study the airway exposure to silica coated TiO_2 NP, but not to the pristine one, induced pulmonary neutrophilia in BALB/c mice with concomitant increase of expression of tumor necrosis factor-alpha and neutrophil-attracting chemokine CXCL1 in the lung tissue (53). Conversely, in rats intratracheally instilled with silica and alumina surface coated TiO_2 NP, a lower induction of adverse pulmonary health effects respect to uncoated NP was observed (54). *In vitro*, silica-coating improved the biocompatibility of TiO_2 NP in a mouse fibroblast cell line (55) while in dorsal root ganglion cells after exposure to several types of TiO_2 NP, among which two NP coated with silica, NP induced apoptosis with the only exception of the uncoated rutile TiO_2 (56).

Our results, taken together with the conflicting results reported in literature about TiO_2 and ZrO_2 NP toxicity, suggest that integrated testing strategies are required for an adequate assessment of the impact of NP on human health and the environment. It is important, when assessing the hazard associated with NP, to establish standard testing procedures and thorough strategies to consider the different conditions relevant to possible exposures (57,58).

Conclusions

In Table 4, we report a summary of the results obtained with the various endpoints studied, by taking into account comparable doses and time treatment of the NP tested.

From this table, it is evident that each NP is able to induce some toxic effects, although none of the nanomaterials tested is able to induce significant effects for all toxic endpoint investigated.

The NP remediation strategy adopted in this study did not prove to change the toxic effects induced by pristine NP, although the coating with SiO_2 seems to prevent Balb/3T3 morphological transformation induced by ZrO_2 NP. In order to identify any potential impact of NP on human health, it is essential to fully investigate their toxicological profiles in different model systems. A test battery designed to evaluate risks to human health of NP should include reliable test assays, with no NP interferences, that are able to give complementary information on the mechanisms of NP toxicity.

Funding

This study was financially supported by the FP7 projects No CP-FP 214478-2, NanoReTox and No 280716, SANOWORK.

Acknowledgements

We would like to thank Dr. Paolo Lucchesi (Department of Clinical and Experimental Medicine, University of Pisa) for assistance with TEM images acquisition. The authors are responsible for writing of the article and report no conflicts of financial, consulting and personal interests.

Conflict of interest statement: None declared.

References

1. George, S., Ho, S. S., Wong, E. S., *et al.* (2015) The multi-facets of sustainable nanotechnology - Lessons from a nanosafety symposium. *Nanotoxicology*, 9, 404–406.
2. Heiligtag, F. J. and Niederberger, M. (2013) The fascinating world of nanoparticle research. *Materialstoday*, 16, 262–271.
3. Kumar, A. and Dhawan, A. (2013) Genotoxic and carcinogenic potential of engineered nanoparticles: an update. *Arch. Toxicol.*, 87, 1883–1900.
4. Migliore, L., Ubaldi, C., Di Buccianico, S. and Coppedè, F. (2015) Nanomaterials and neurodegeneration. *Environ. Mol. Mutagen.*, 56, 149–170.
5. Nel, A. E., Mädler, L., Velegol, D., Xia, T., Hoek, E. M., Somasundaran, P., Klaessig, F., Castranova, V. and Thompson, M. (2009) Understanding biophysicochemical interactions at the nano-bio interface. *Nat. Mater.*, 8, 543–557.
6. Kurzepa, H., Kyriazis, A. P. and Lang, D. R. (1984) Growth characteristics of tumors induced by transplantation into athymic mice of BALB/3T3 cells transformed *in vitro* by residue organics from drinking water. *J. Environ. Pathol. Toxicol. Oncol.*, 5, 131–138.

7. Saffiotti, U. and Ahmed, N. (1995) Neoplastic transformation by quartz in the BALB/3T3/A31-1-1 cell line and the effects of associated minerals. *Teratog. Carcinog. Mutagen.*, 15, 339–356.
8. Ortelli, S., Blosi, M., Albonetti, S., Vaccari, A., Dondi, M. and Costa, A. L. (2013) TiO₂ based nano-photocatalysis immobilized on cellulose substrates. *J. Photochem. Photobiol. A: Chem.*, 276, 58–64.
9. Brunauer, S., Emmett, P. H. and Teller E. (1938) Adsorption of gases in multimolecular layers. *J. Am. Chem. Soc.*, 60, 309–319.
10. Brunauer, S., Deming, L. S., Deming, W. E. and Teller, E. (1940) On a theory of the van der Waals adsorption of gases. *J. Am. Chem. Soc.*, 62, 1723–1732.
11. Gangwal, S., Brown, J. S., Wang, A., Houck, K. A., Dix, D. J., Kavlock, R. J. and Hubal, E. A. (2011) Informing selection of nanomaterial concentrations for ToxCast in vitro testing based on occupational exposure potential. *Environ. Health Perspect.*, 119, 1539–1546.
12. Ponti, J., Broggi, F., Mariani, V., et al. (2013) Morphological transformation induced by multiwall carbon nanotubes on Balb/3T3 cell model as an in vitro end point of carcinogenic potential. *Nanotoxicology*, 7, 221–233.
13. ENV/JM/MONO(2011)30 of 06-Feb-2012 BALB/C 3T3 cell transformation assay prevalidation study report. Series on Testing and Assessment No. 149. [http://www.oecd.org/officialdocuments/publicdisplaydocumentpdf/?cote=ENV/JM/MONO\(2011\)30&doclang=eng](http://www.oecd.org/officialdocuments/publicdisplaydocumentpdf/?cote=ENV/JM/MONO(2011)30&doclang=eng)
14. Uboldi, C., Giudetti, G., Broggi, F., Gilliland, D., Ponti, J. and Rossi, F. (2012) Amorphous silica nanoparticles do not induce cytotoxicity, cell transformation or genotoxicity in Balb/3T3 mouse fibroblasts. *Mutat. Res.*, 745, 11–20.
15. Di Buccianico, S., Fabbri, M. R., Misra, S. K., Valsami-Jones, E., Berhanu, D., Reip, P., Bergamaschi, E. and Migliore, L. (2013) Multiple cytotoxic and genotoxic effects induced in vitro by differently shaped copper oxide nanomaterials. *Mutagenesis*, 28, 287–299.
16. Fenech, M. (2007) Cytokinesis-block micronucleus cytome assay. *Nat. Protoc.*, 2, 1084–1104.
17. Rezwan, K., Studart, A. R., Vörös, J. and Gauckler, L. J. (2005) Change of zeta potential of biocompatible colloidal oxide particles upon adsorption of bovine serum albumin and lysozyme. *J. Phys. Chem. B*, 109, 14469–14474.
18. Lynch, I. and Dawson, K. A. (2008) Protein-nanoparticle interactions. *Nanotoday*, 3, 40–47.
19. Song, L., Yang, K., Jiang, W., Du, P. and Xing, B. (2012) Adsorption of bovine serum albumin on nano and bulk oxide particles in deionized water. *Colloids Surf. B: Biointerfaces*, 94, 341–346.
20. Ponti, J., Ceriotti, L., Munaro, B., Farina, M., Munari, A., Whelan, M., Colpo, P., Sabbioni, E. and Rossi, F. (2006) Comparison of impedance-based sensors for cell adhesion monitoring and in vitro methods for detecting cytotoxicity induced by chemicals. *Altern. Lab. Anim.*, 34, 515–525.
21. Soto, K., Garza, K. M. and Murr, L. E. (2007) Cytotoxic effects of aggregated nanomaterials. *Acta Biomater.*, 3, 351–358.
22. Demir, E., Burgucu, D., Turna, F., Aksakal, S. and Kaya, B. (2013) Determination of TiO₂, ZrO₂, and Al₂O₃ nanoparticles on genotoxic responses in human peripheral blood lymphocytes and cultured embryonic kidney cells. *J. Toxicol. Environ. Health. A*, 76, 990–1002.
23. Dalal, A., Pawar, V., McAllister, K., Weaver, C. and Hallab, N. J. (2012) Orthopedic implant cobalt-alloy particles produce greater toxicity and inflammatory cytokines than titanium alloy and zirconium alloy-based particles in vitro, in human osteoblasts, fibroblasts, and macrophages. *J. Biomed. Mater. Res. A*, 100, 2147–2158.
24. Karunakaran, G., Suriyapratha, R., Manivasakan, P., Yuvakkumar, R., Rajendran, V. and Kannan, N. (2013) Screening of in vitro cytotoxicity, antioxidant potential and bioactivity of nano- and micro-ZrO₂ and -TiO₂ particles. *Ecotoxicol. Environ. Saf.*, 93, 191–197.
25. Lanone, S., Rogerieux, F., Geys, J., Dupont, A., Maillot-Marechal, E., Boczkowski, J., Lacroix, G. and Hoet, P. (2009) Comparative toxicity of 24 manufactured nanoparticles in human alveolar epithelial and macrophage cell lines. *Part. Fibre Toxicol.*, 30, 6–14.
26. Falck, G. C., Lindberg, H. K., Suhonen, S., Vippola, M., Vanhala, E., Catalán, J., Savolainen, K. and Norppa, H. (2009) Genotoxic effects of nano-sized and fine TiO₂. *Hum. Exp. Toxicol.*, 28, 339–352.
27. Bhattacharya, K., Davoren, M., Boertz, J., Schins, R. P., Hoffmann, E. and Dopp, E. (2009) Titanium dioxide nanoparticles induce oxidative stress and DNA-adduct formation but not DNA-breakage in human lung cells. *Part. Fibre Toxicol.*, 21, 6–17.
28. Montiel-Dávalos, A., Ventura-Gallegos, J. L., Alfaro-Moreno, E., Soria-Castro, E., García-Latorre, E., Cabañas-Moreno, J. G., del Pilar Ramos-Godínez, M. and López-Marure, R. (2012) TiO₂ nanoparticles induce dysfunction and activation of human endothelial cells. *Chem. Res. Toxicol.*, 25, 920–930.
29. Márquez-Ramírez, S. G., Delgado-Buenrostro, N. L., Chirino, Y. I., Iglesias, G. G. and López-Marure, R. (2012) Titanium dioxide nanoparticles inhibit proliferation and induce morphological changes and apoptosis in glial cells. *Toxicology*, 302, 146–156.
30. Guichard, Y., Schmit, J., Darne, C., et al. (2012) Cytotoxicity and genotoxicity of nanosized and microsized titanium dioxide and iron oxide particles in Syrian hamster embryo cells. *Ann. Occup. Hyg.*, 56, 631–644.
31. Hackenberg, S., Friehs, G., Kessler, M., Froelich, K., Ginzkey, C., Koehler, C., Scherzed, A., Burghartz, M. and Kleinsasser, N. (2011) Nanosized titanium dioxide particles do not induce DNA damage in human peripheral blood lymphocytes. *Environ. Mol. Mutagen.*, 52, 264–268.
32. Petković, J., Zegura, B., Stevanović, M., Drnovšek, N., Uskoković, D., Novak, S. and Filipič, M. (2011) DNA damage and alterations in expression of DNA damage responsive genes induced by TiO₂ nanoparticles in human hepatoma HepG2 cells. *Nanotoxicology*, 5, 341–353.
33. Jugan, M. L., Barillet, S., Simon-Deckers, A., Herlin-Boime, N., Sauvaigo, S., Douki, T. and Carriere, M. (2012) Titanium dioxide nanoparticles exhibit genotoxicity and impair DNA repair activity in A549 cells. *Nanotoxicology*, 6, 501–513.
34. Kroll, A., Pillukat, M. H., Hahn, D. and Schnekenburger, J. (2012) Interference of engineered nanoparticles with in vitro toxicity assays. *Arch. Toxicol.*, 86, 1123–1136.
35. Lupu, A. R. and Popescu, T. (2013) The noncellular reduction of MTT tetrazolium salt by TiO₂ nanoparticles and its implications for cytotoxicity assays. *Toxicol. In Vitro*, 27, 1445–1450.
36. Ponti, J., Kinsner-Ovaskainen, A., Norlén, H., Altmeyer, S., et al. (2014) Interlaboratory comparison study of the colony forming efficiency assay for assessing cytotoxicity of nanomaterials. *EUR*.
37. Tavares, A. M., Louro, H., Antunes, S., et al. (2014) Genotoxicity evaluation of nanosized titanium dioxide, synthetic amorphous silica and multi-walled carbon nanotubes in human lymphocytes. *Toxicol. In Vitro*, 28, 60–69.
38. Osman, I. F., Baumgartner, A., Cemeli, E., Fletcher, J. N. and Anderson, D. (2010) Genotoxicity and cytotoxicity of zinc oxide and titanium dioxide in HEp-2 cells. *Nanomedicine (Lond.)*, 5, 1193–1203.
39. Demir, E., Akça, H., Turna, F., et al. (2015) Genotoxic and cell-transforming effects of titanium dioxide nanoparticles. *Environ. Res.*, 136, 300–308.
40. Prasad, R. Y., Wallace, K., Daniel, K. M., et al. (2013) Effect of treatment media on the agglomeration of titanium dioxide nanoparticles: impact on genotoxicity, cellular interaction, and cell cycle. *ACS Nano*, 7, 1929–1942.
41. Rahman, Q., Lohani, M., Dopp, E., Pemsel, H., Jonas, L., Weiss, D. G. and Schiffmann, D. (2002) Evidence that ultrafine titanium dioxide induces micronuclei and apoptosis in Syrian hamster embryo fibroblasts. *Environ. Health Perspect.*, 110, 797–800.
42. Gurr, J. R., Wang, A. S., Chen, C. H. and Jan, K. Y. (2005) Ultrafine titanium dioxide particles in the absence of photoactivation can induce oxidative damage to human bronchial epithelial cells. *Toxicology*, 213, 66–73.
43. Demir, E., Turna, F., Vales, G., Kaya, B., Creus, A. and Marcos, R. (2013) In vivo genotoxicity assessment of titanium, zirconium and aluminium nanoparticles, and their microparticulated forms, in *Drosophila*. *Chemosphere*, 93, 2304–2310.
44. Hackenberg, S., Friehs, G., Froelich, K., Ginzkey, C., Koehler, C., Scherzed, A., Burghartz, M., Hagen, R. and Kleinsasser, N. (2010) Intracellular distribution, geno- and cytotoxic effects of nanosized titanium dioxide particles in the anatase crystal phase on human nasal mucosa cells. *Toxicol. Lett.*, 195, 9–14.
45. Huk, A., Izak-Nau, E., Reidy, B., Boyles, M., Duschl, A., Lynch, I. and Dušinska, M. (2014) Is the toxic potential of nanosilver dependent on its size? *Part. Fibre Toxicol.*, 3, 11–65.
46. Hartung, T., Bremer, S., Casati, S., et al. (2003) ECVAM's response to the changing political environment for alternatives: consequences of the European Union chemicals and cosmetics policies. *Altern. Lab. Anim.*, 31, 473–481.
47. Maccauro, G., Bianchino, G., Sangiorgi, S., et al. (2009) Development of a new zirconia-toughened alumina: promising mechanical properties and absence of in vitro carcinogenicity. *Int. J. Immunopathol. Pharmacol.*, 22, 773–779.

48. Covacci, V., Bruzzese, N., Maccauro, G., Andreassi, C., Ricci, G. A., Piconi, C., Marmo, E., Burger, W. and Cittadini, A. (1999) In vitro evaluation of the mutagenic and carcinogenic power of high purity zirconia ceramic. *Biomaterials*, 20, 371–376.
49. IARC. (2010) *Carbon black, titanium dioxide, and talc*.
50. Vales, G., Rubio, L. and Marcos, R. (2014) Long-term exposures to low doses of titanium dioxide nanoparticles induce cell transformation, but not genotoxic damage in BEAS-2B cells. *Nanotoxicology*, 19, 1–11.
51. Huang, S., Chueh, P. J., Lin, Y. W., Shih, T. S. and Chuang, S. M. (2009) Disturbed mitotic progression and genome segregation are involved in cell transformation mediated by nano-TiO₂ long-term exposure. *Toxicol. Appl. Pharmacol.*, 241, 182–194.
52. Huk, A., Izak-Nau, E., El Yamani, N., Uggerud, H., Vadset, M., Zasonska, B., Duschl, A. and Dusinska, M. (2015) Impact of nanosilver on various DNA lesions and HPRT gene mutations - effects of charge and surface coating. *Part. Fibre Toxicol.* 24, 12–25.
53. Rossi, E. M., Pylkkänen, L., Koivisto, A. J., *et al.* (2010) Airway exposure to silica-coated TiO₂ nanoparticles induces pulmonary neutrophilia in mice. *Toxicol. Sci.*, 113, 422–433.
54. Warheit, D. B., Webb, T. R., Reed, K. L., Frerichs, S. and Sayes, C. M. (2007) Pulmonary toxicity study in rats with three forms of ultrafine-TiO₂ particles: differential responses related to surface properties. *Toxicology*, 230, 90–104.
55. Feng, X., Zhang, S. and Lou, X. (2013) Controlling silica coating thickness on TiO₂ nanoparticles for effective photodynamic therapy. *Colloids Surf. B. Biointerfaces*, 107, 220–226.
56. Bolis, V., Busco, C., Ciarletta, M., Distasi, C., Erriquez, J., Fenoglio, I., Livraghi, S. and Morel, S. (2012) Hydrophilic/hydrophobic features of TiO₂ nanoparticles as a function of crystal phase, surface area and coating, in relation to their potential toxicity in peripheral nervous system. *J. Colloid Interface Sci.*, 369, 28–39.
57. Farcal, L., Torres Andón, F., Di Cristo, L., *et al.* (2015) Comprehensive In Vitro Toxicity Testing of a Panel of Representative Oxide Nanomaterials: First Steps towards an Intelligent Testing Strategy. *PLoS One*, 10, e0127174.
58. Oomen, A. G., Bos, P. M., Fernandes, T. F., *et al.* (2014) Concern-driven integrated approaches to nanomaterial testing and assessment—report of the NanoSafety Cluster Working Group 10. *Nanotoxicology*, 8, 334–348.